Recent Photon and Jet QCD Results from the Tevatron

Prompt diphoton production (DØ, CDF)
High transverse momentum jets (CDF)
Multiple parton interactions (DØ)

Susan Blessing
Florida State University

For the DØ and CDF Collaborations

23rd Rencontres de Blois
June 1, 2011

Prompt diphoton production (DØ and CDF)

Prompt photons are produced directly from the hard-scattering or fragmentation process

as opposed to photons from π^0, η, K_s^0 decay

At a much smaller rate, < 1%, photon pairs may come from Higgs decay, graviton decay (extra dimensions), neutralino decay (SUSY)

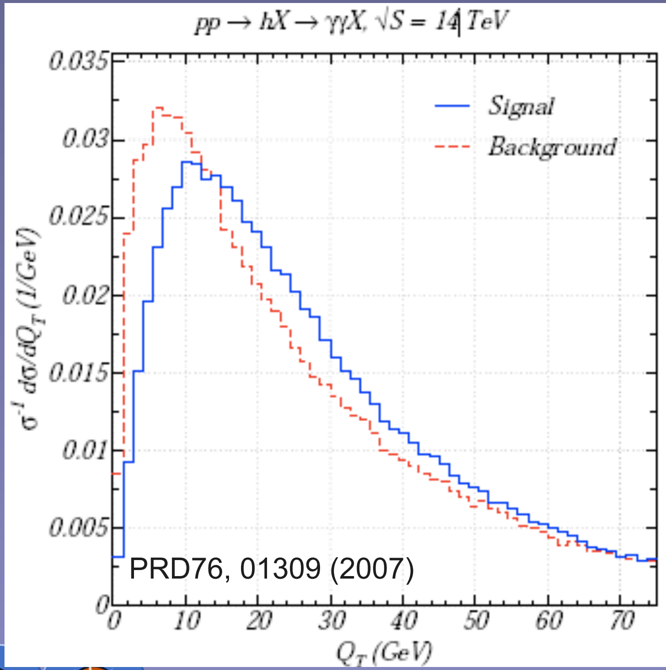

gg → H → γγ is the main discovery channel for Higgs up to about 130 GeV at LHC

QCD γγ and H → γγ have different dominant initial states – $q\bar{q}$ vs. gg

Leads to differences in kinematic distributions

Prompt diphoton production

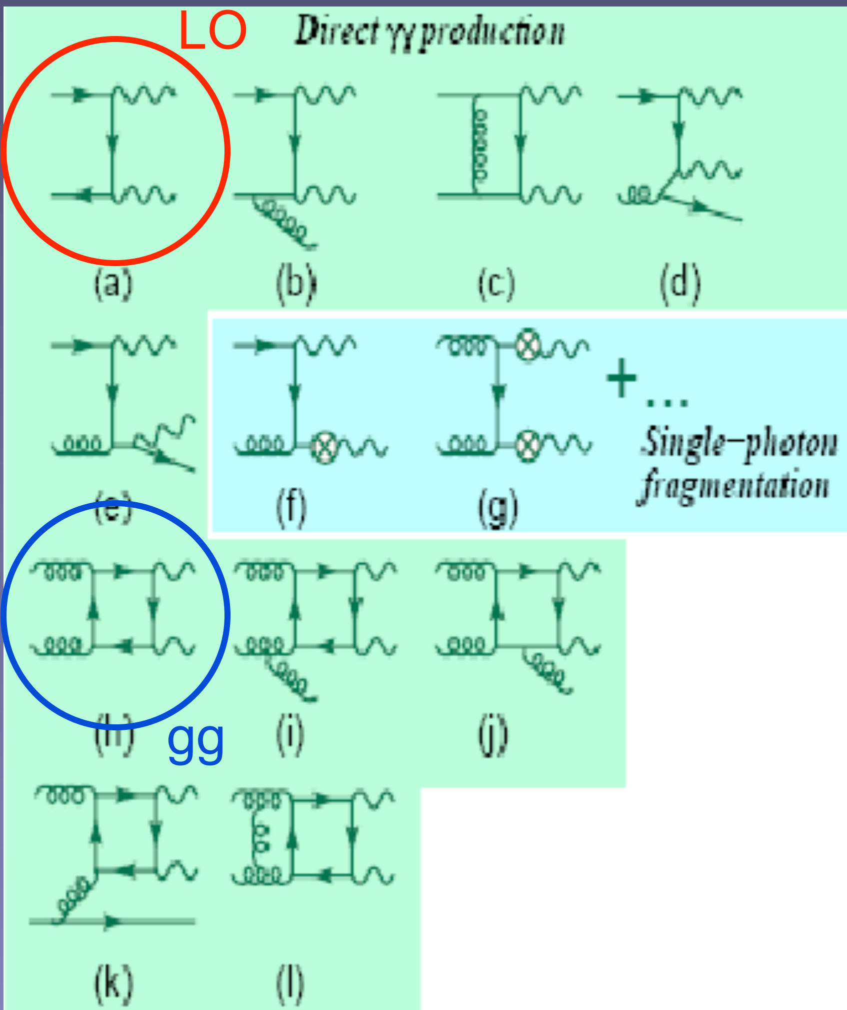

Two primary production mechanisms
direct and fragmentation

Direct

At LO – $q\bar{q}$ scattering only
At NLO –
virtual corrections, real emissions
gg scattering – $O(\alpha_s^2)$ suppression
but large gluon PDF makes for a significant contribution at low $M_{\gamma\gamma}$

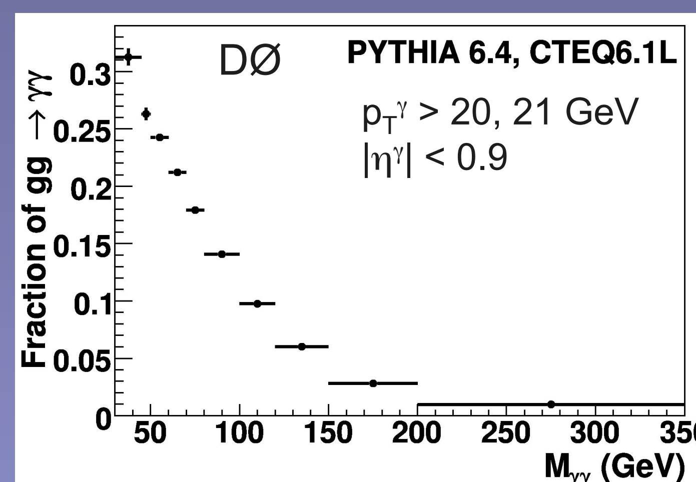

Prompt diphoton production

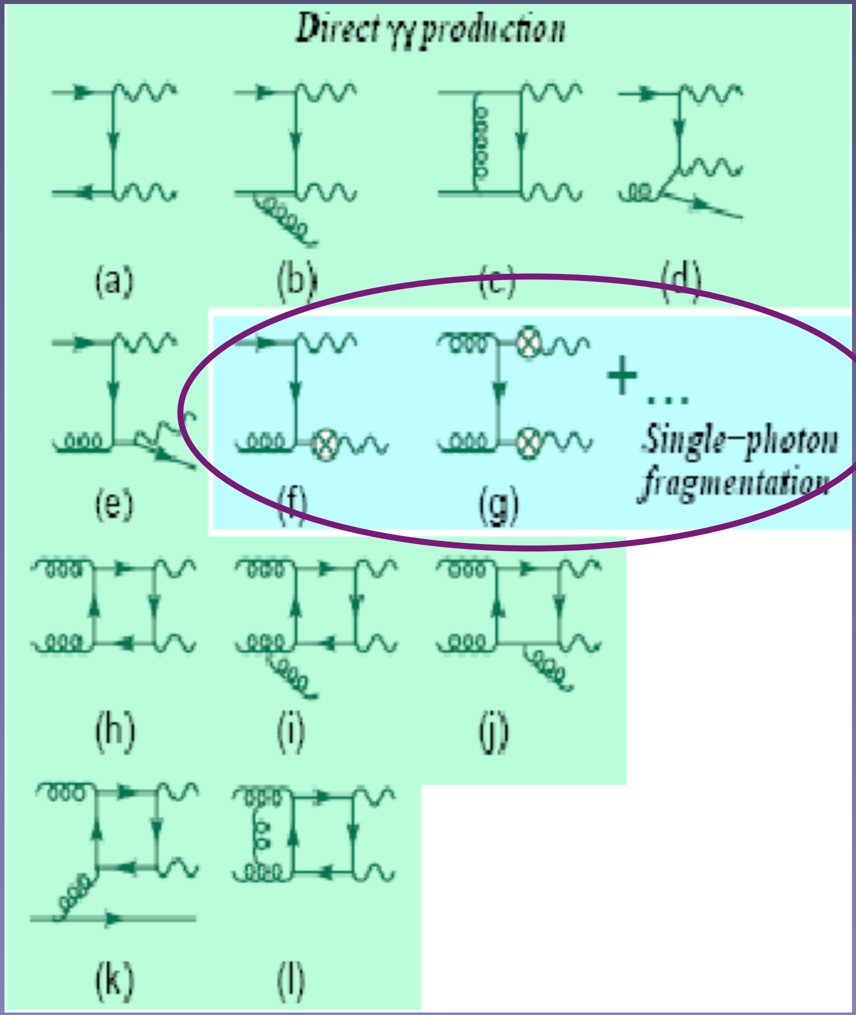

Fragmentation

Enhances cross section in some kinematic regions

depends on photon selections

Collinear singularities are factored out into fragmentation functions $D_{\gamma/q}$

Fragmentation contribution is very uncertain and can be suppressed experimentally by requiring

- isolated photons
- $p_T^{\gamma\gamma} < M_{\gamma\gamma}$ [PRD 76, 013009 (2007)]

Predictions

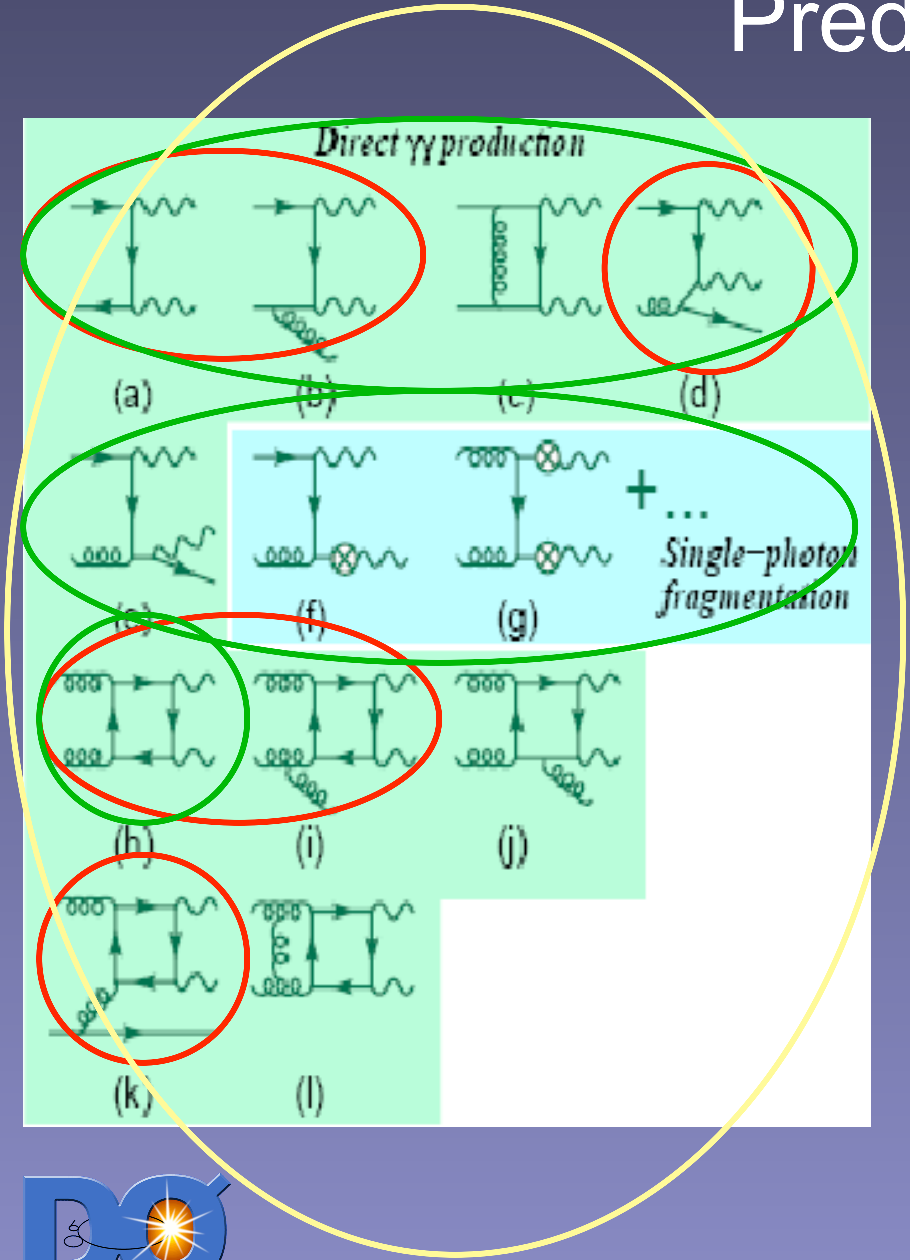

PYTHIA [JHEP 05, 026 (2006)]

- $q\bar{q} \to \gamma\gamma$ and $gg \to \gamma\gamma$ matrix elements
- All-order resummation to LL accuracy
- No fragmentation photons
- Diagrams a, b, d, h, i, k

DIPHOX [EPJ C16, 311 (2000)]

- Fixed-order NLO calculation
  ($gg \to \gamma\gamma$ is at LO)
- No soft gluon resummation
- Single photon fragmentation at NLO
- Diagrams a, b, c, d, e, f, g, h

RESBOS [PRD 76, 01309 (2007)]

- NLO $q\bar{q} \to \gamma\gamma$ and $gg \to \gamma\gamma$
- All-orders initial soft gluon resummation to NNLL accuracy
- $2m_b < M_{\gamma\gamma} < 2m_t$
- Single photon fragmentation included as a parameterization
- Diagrams a, b, c, d, e, f, g, h, i, j, k, l

Event selection

DØ – 4.2 fb^{-1} [PLB 690, 108 (2010)]

- Two photons, p_T > 20, 21 GeV, $|\eta_\gamma|$ < 0.9
- Separated by $\Delta R_{\gamma\gamma}$ > 0.4
- $p_T^{\gamma\gamma} < M_{\gamma\gamma}$ (suppress fragmentation)
- EM fraction > 0.97
- Isolated, calorimeter and tracker
- Photon neural net
  (cal, preshower, tracking info)

CDF – 5.36 fb^{-1} [Preliminary]

- Two photons, E_T > 15,17 GeV, $|y_\gamma|$ < 1
- Separated by $\Delta R_{\gamma\gamma}$ > 0.4
- Isolated, calorimeter and tracker
- With and without $p_T^{\gamma\gamma} < M_{\gamma\gamma}$
  - large and small $\Delta\phi_{\gamma\gamma}$ (not shown here)

- Typical diphoton purity ~70%
- Main backgrounds
  - γ + jet (~15%)
  - dijet (~15%)
  - $Z/\gamma^* \rightarrow ee$ (~2%)

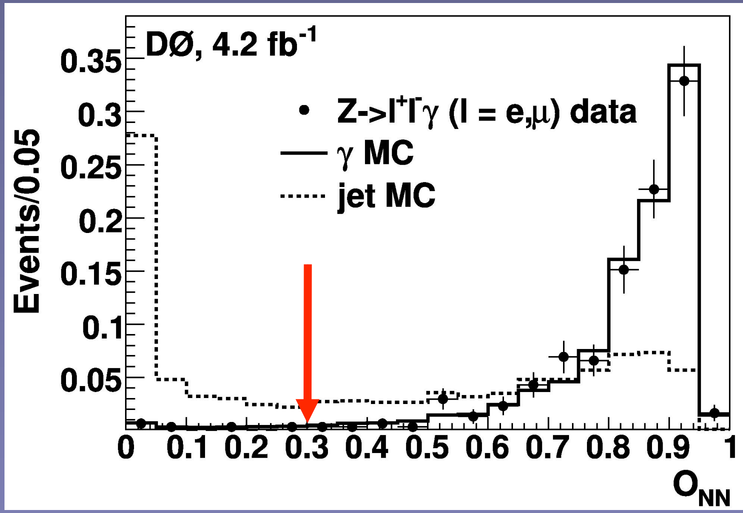

Photon neural net output

Good discrimination – EM jets/photons
Good agreement – data/γ MC

Measurements

Single differential cross sections shown

Sensitive to ISR and fragmentation

$$\frac{d\sigma}{dM_{\gamma\gamma}} \qquad \frac{d\sigma}{dp_T^{\gamma\gamma}} \qquad \frac{d\sigma}{d\Delta\phi_{\gamma\gamma}}$$

Sensitive to PDFs

$$\frac{d\sigma}{d|\cos\theta^*|}$$

Sensitive to energy scale of the interaction and new physics

Double differential cross section shown

$$\frac{d^2\sigma}{dM_{\gamma\gamma}\, dp_T^{\gamma\gamma}} \begin{cases} 30 \leq M_{\gamma\gamma} < 50 \text{ GeV} \\ 50 \leq M_{\gamma\gamma} < 80 \text{ GeV} \\ 80 \leq M_{\gamma\gamma} < 350 \text{ GeV} \end{cases}$$

Both collaborations have measured additional single differential cross sections. DØ has measured two additional double differential cross sections.

Effect of $p_T^{\gamma\gamma} < M_{\gamma\gamma}$ – CDF

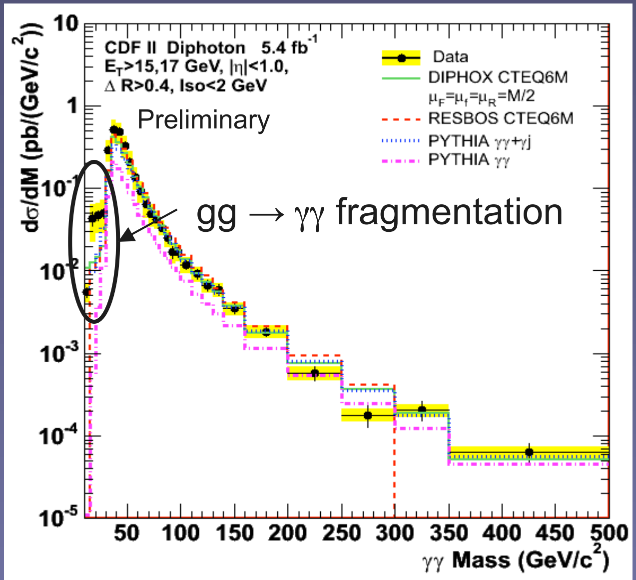

No $p_T^{\gamma\gamma}$ cut

$$\frac{d\sigma}{dM_{\gamma\gamma}}$$

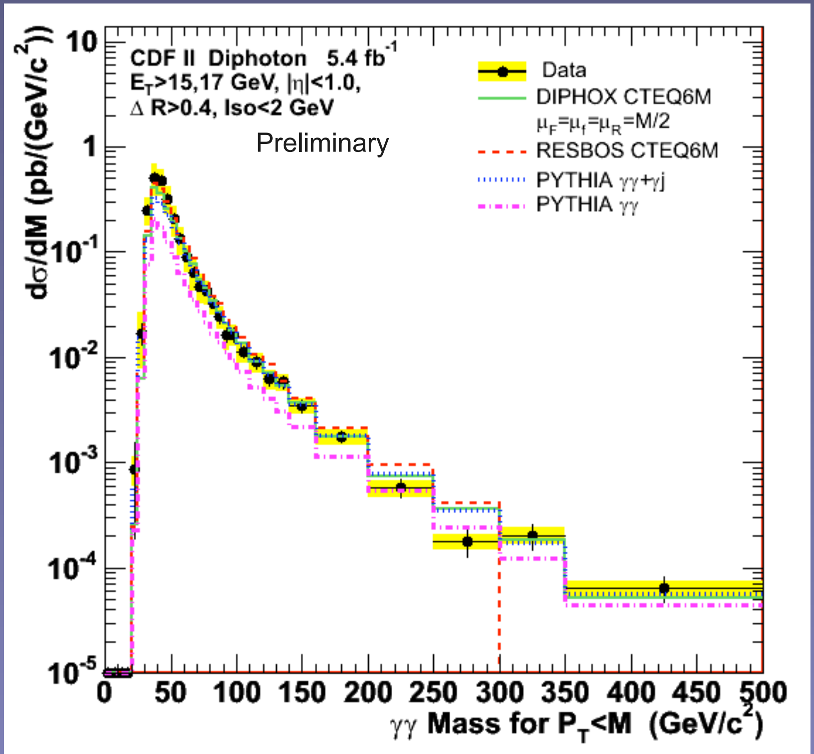

$p_T^{\gamma\gamma} < M_{\gamma\gamma}$

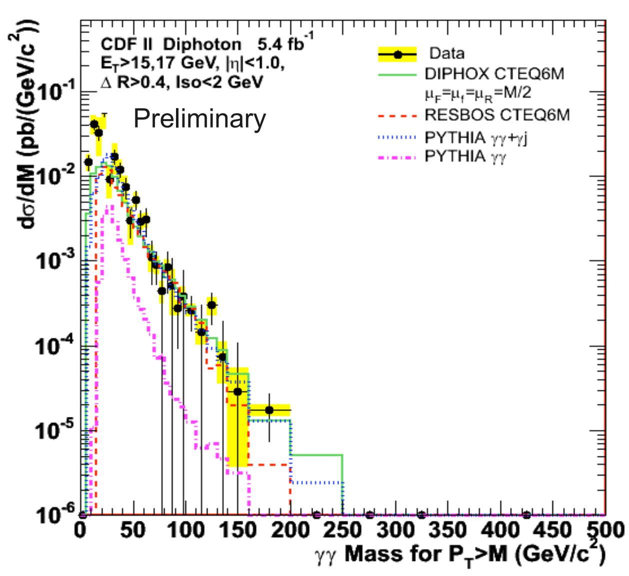

$p_T^{\gamma\gamma} > M_{\gamma\gamma}$

$$\frac{d\sigma}{dM_{\gamma\gamma}}$$

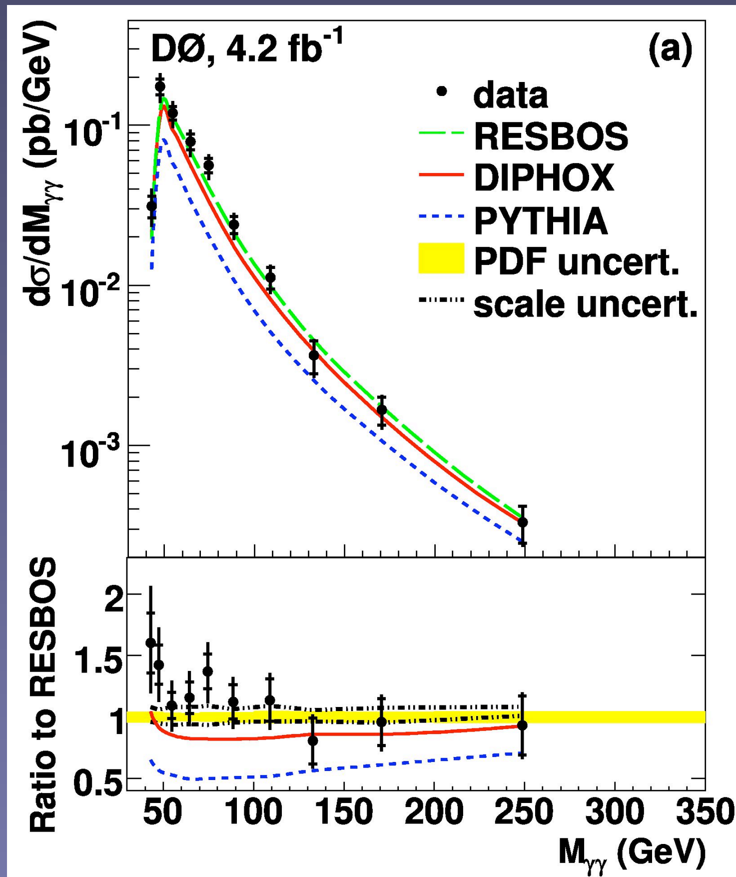

Good agreement between data and RESBOS for $M_{\gamma\gamma}$ > 50 GeV

DØ
PLB 690, 108 (2010)

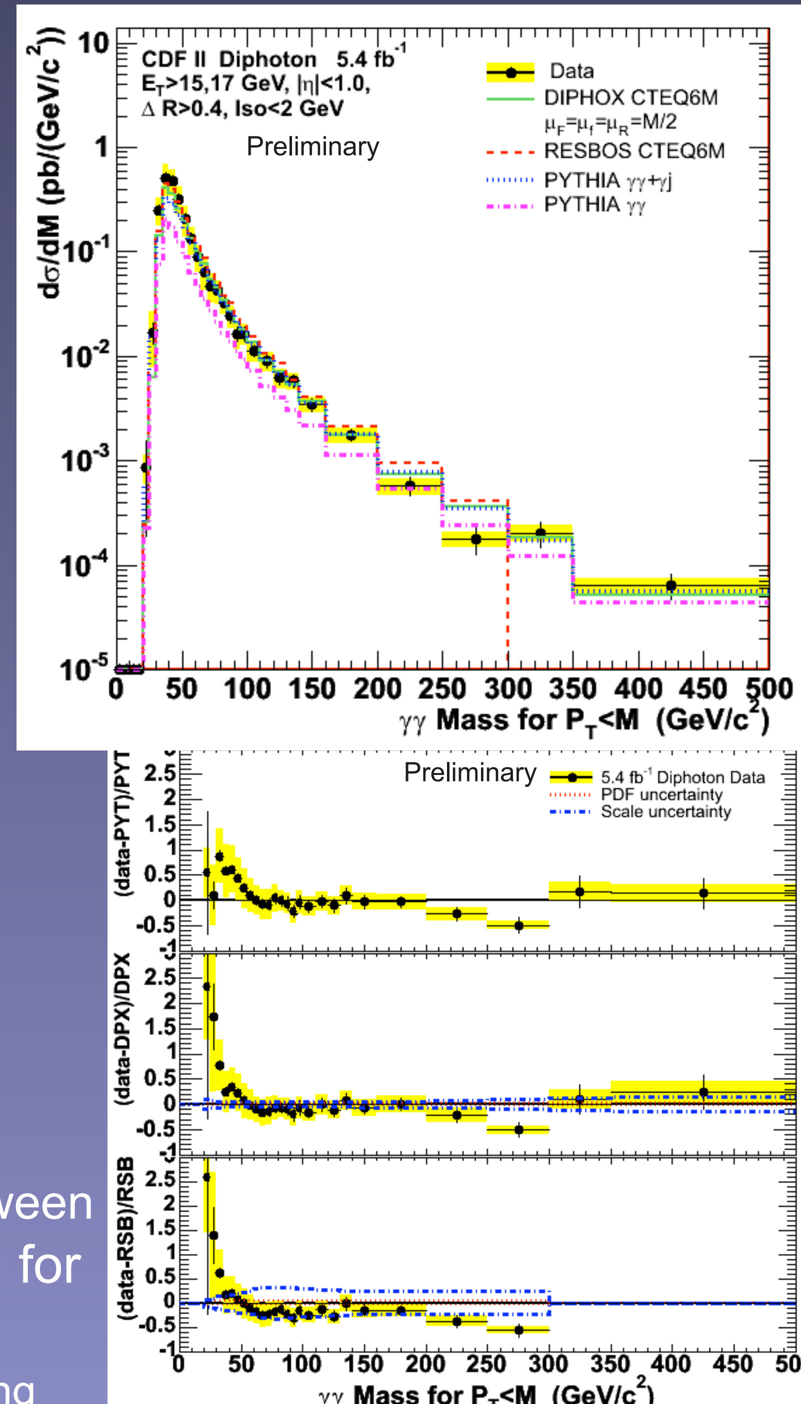

Best agreement is between data and PYTHIA $\gamma\gamma+\gamma j$ for $M_{\gamma\gamma}$ > 60 GeV

Susan Blessing

$$\frac{d\sigma}{dp_T^{\gamma\gamma}}$$

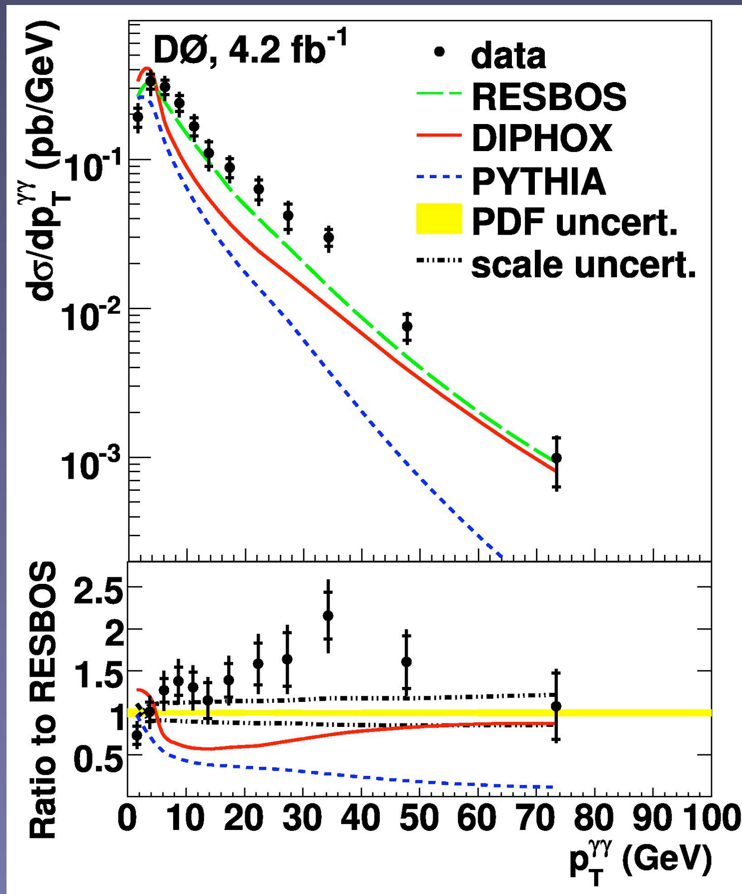

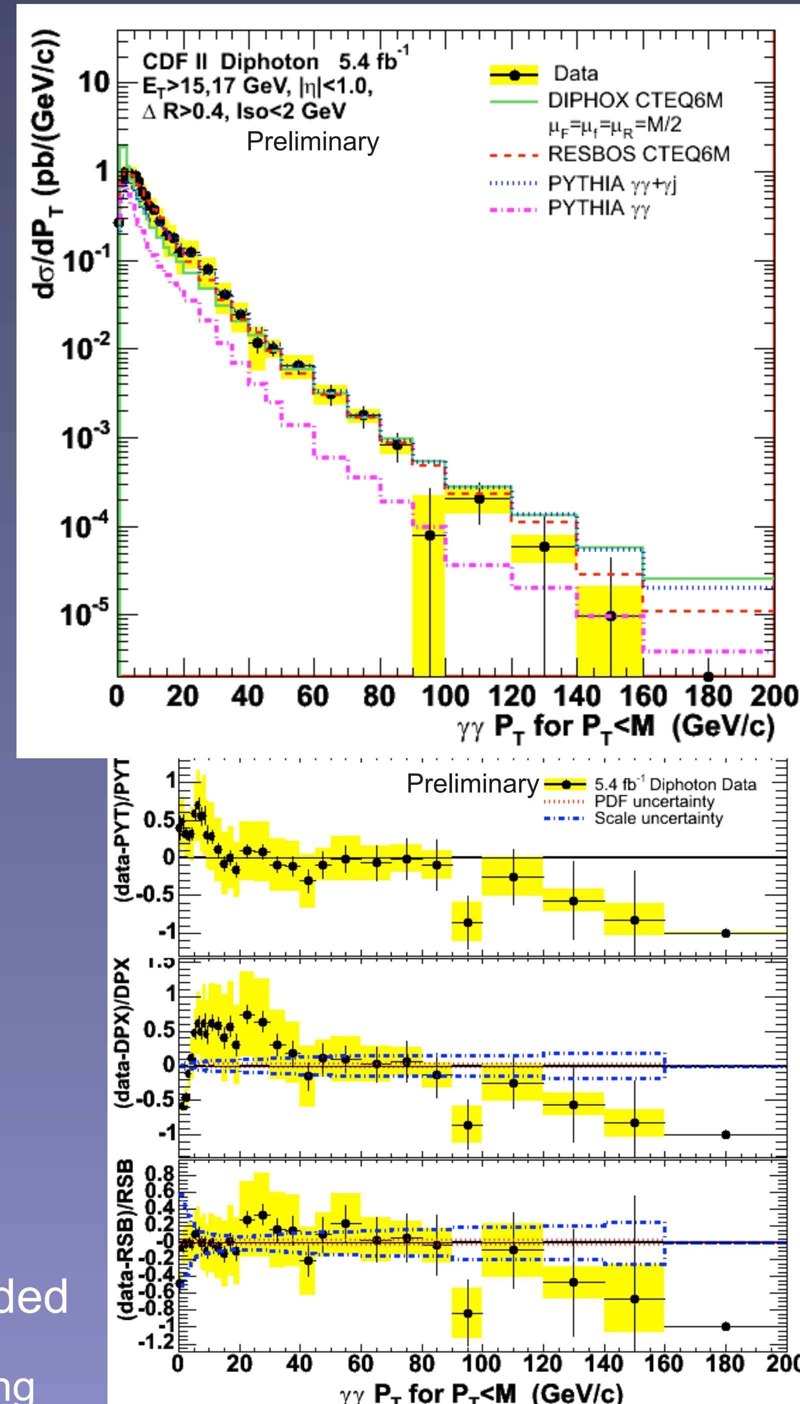

Data spectrum harder than predicted

Need NNLO?

Discrepancy with DIPHOX and PYTHIA at small $p_T^{\gamma\gamma}$ indicates soft gluon resummation is needed

$$\frac{d\sigma}{d\Delta\phi_{\gamma\gamma}}$$

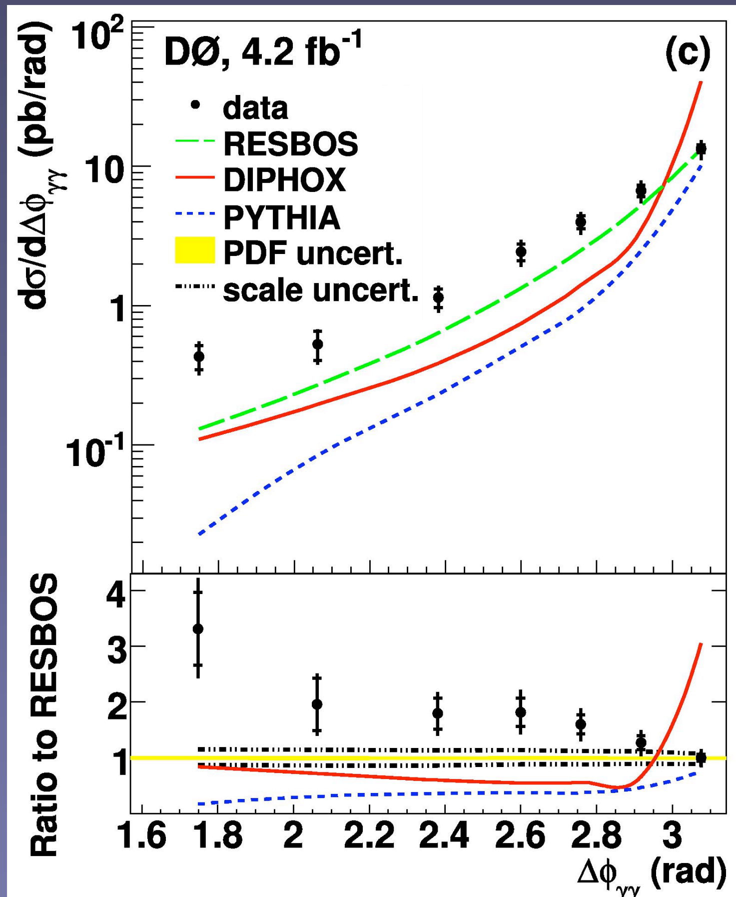

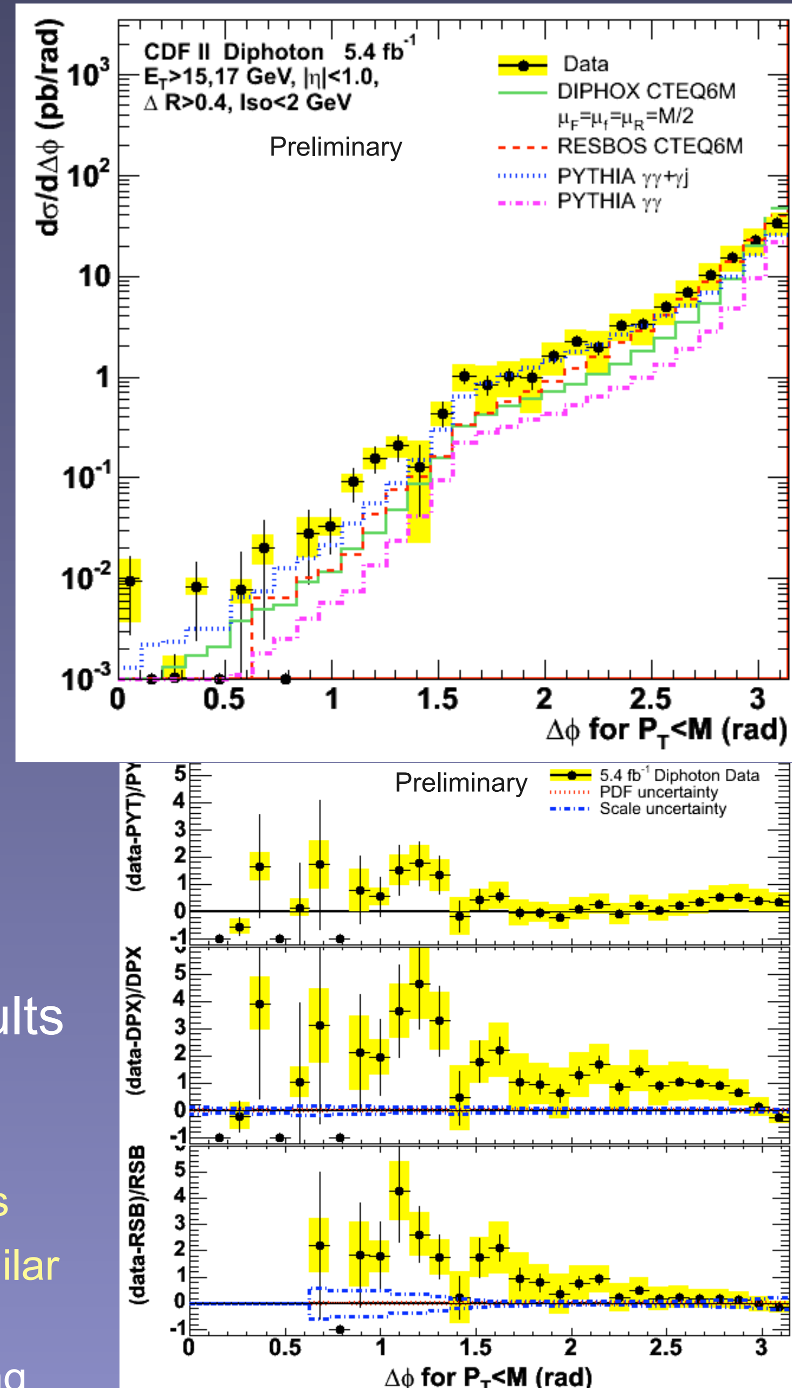

Confirmation of $p_T^{\gamma\gamma}$ results with angular variable

DØ and CDF results are complementary in terms of considered phase space and cross sections

With similar selections, conclusions are similar

Susan Blessing

$\frac{d^2\sigma}{dM_{\gamma\gamma}\, dp_T^{\gamma\gamma}}$ – DØ

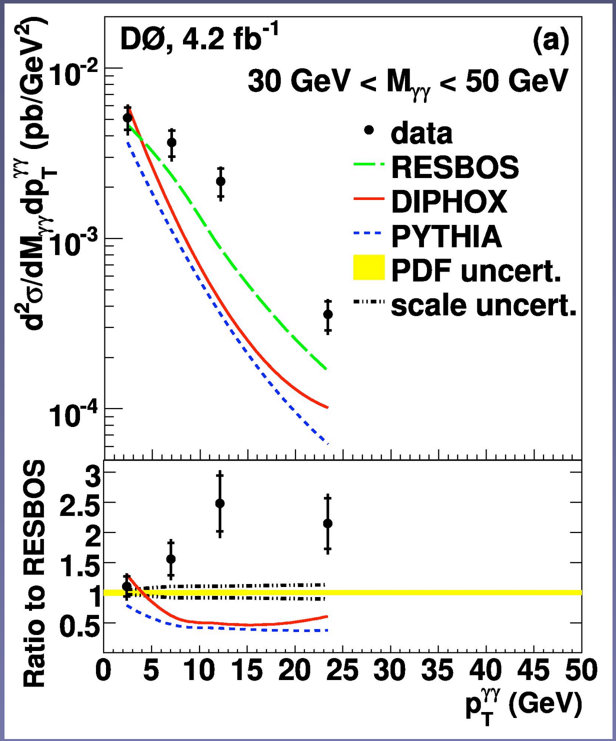

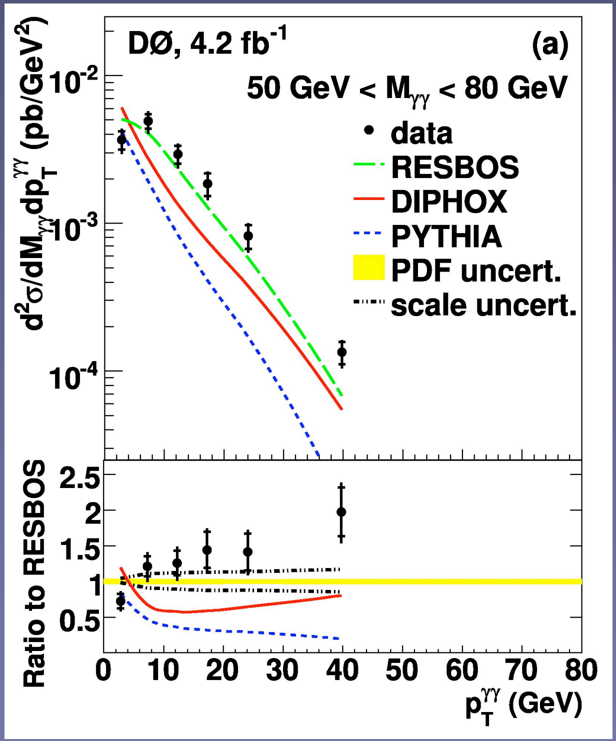

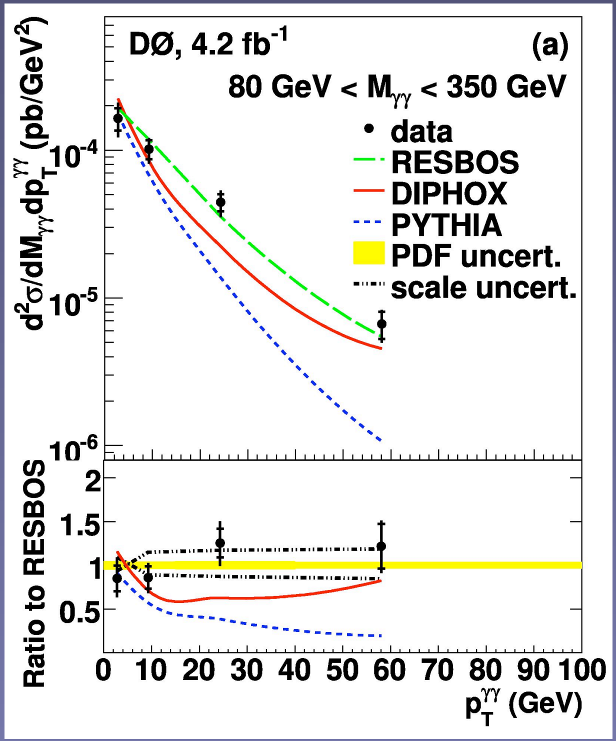

Cross section underestimated as $p_T^{\gamma\gamma}$ increases

Mass region has significant contribution from $gg \rightarrow \gamma\gamma$

Agreement is much better

Improved agreement with RESBOS as $M\gamma\gamma$ increases also seen for $\Delta\phi_{\gamma\gamma}$, $|\cos\theta^*|$

Good agreement with RESBOS at high $M_{\gamma\gamma}$

Mass region important for Higgs and NP searches

High p_T jets – CDF

6 fb^{-1}

Study the mass of high p_T jets

Study the energy flow within jets

Tune parton showering mechanisms

Background to heavy resonance searches

Mass calculated using the standard E-scheme

- 4-vector sum over towers in a jet
- Gives (E, p_x, p_y, p_z)

Reconstruct jets with midpoint cone algorithm

- R = 0.4, 0.7, 1.0

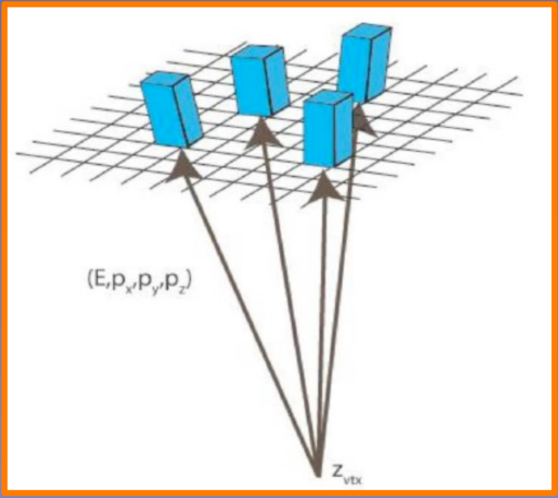

Require

- **≥ 1** jet with $p_T > 400$ GeV, $0.1 < |y_{jet}| < 0.7$
- Reject boosted top quark events
  - $p_T^{jet2} > 100$ GeV
  - $m_{jet2} < 100$ GeV
  - $\not{E}_T / \sum E_T < 4$

2108 events

R = 0.7

Mass distributions

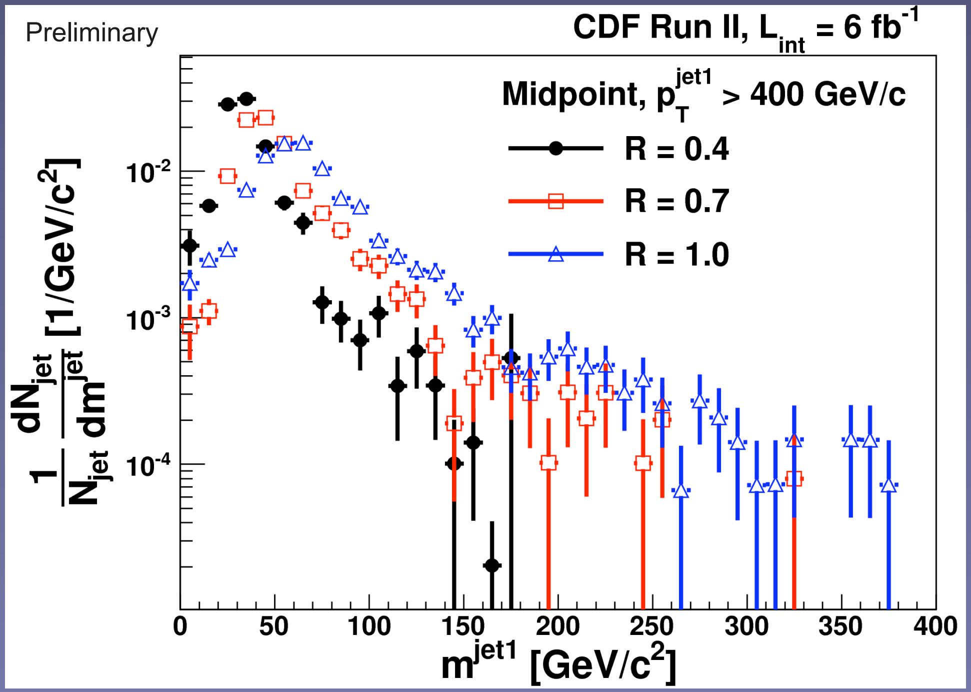

Comparison of m_{jet1} distributions for R = 0.4, 0.7, and 1.0

Cone size plays a clear role in limiting high mass behavior

Jet mass corrected for multiple interactions and the effect of the p_T selection on the jet mass distribution

Mass, R, PYTHIA comparison

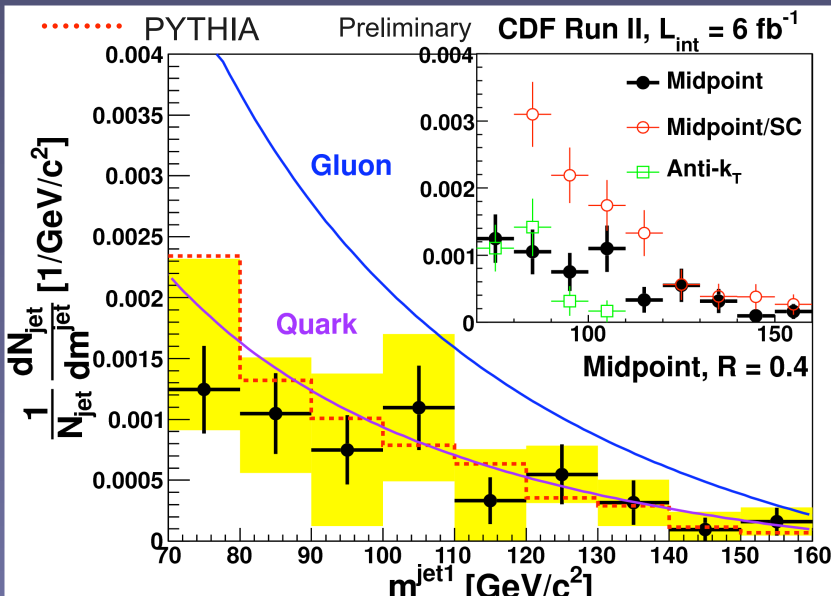

Good agreement between data and PYTHIA prediction over 70 < m_{jet1} < 400 GeV

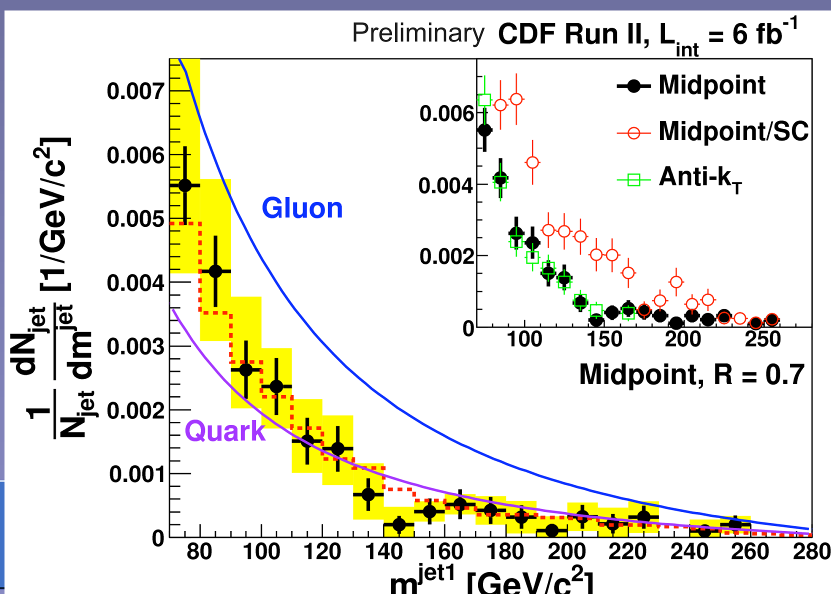

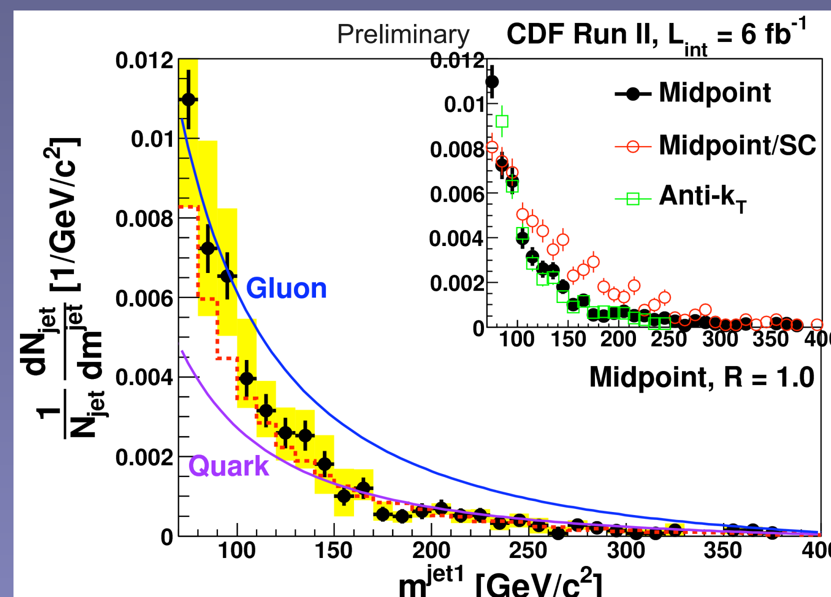

Other jet reconstruction algorithms shown in upper right.
SC = search cone

Angularity

Sensitive to the degree of symmetry in the energy deposition within a jet

Distinguish between jets originating from regular QCD production of light quarks and gluons from boosted heavy particle decay

$$\tau_a(R,p_T) = \frac{1}{m_{jet}} \sum_{i \in jet} \omega_i \sin^a \theta_i \, [1 - \cos \theta_i]^{1-a} \approx \frac{2^{a-1}}{m_{jet}} \sum_{i \in jet} \omega_i \, \theta_i^{2-a}$$

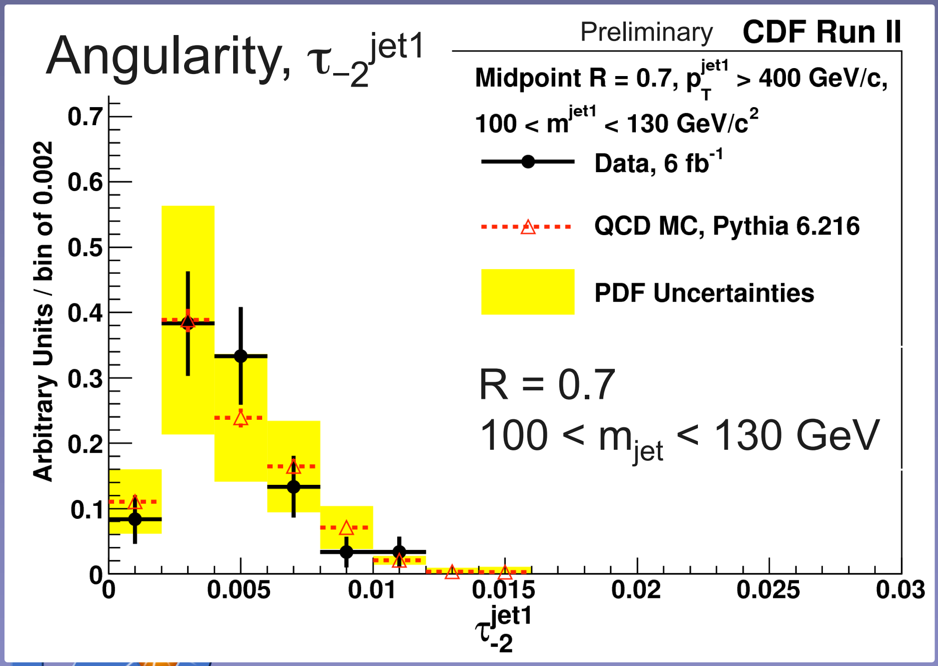

Describes a class of jet shapes

IR safe for a ≤ 2 , a = −2 here

Sum over calorimeter towers in jet

ω_i – energy of a jet tower (particle)

Large = energy at edge of cone ≈ QCD-jet-like

Small = energy at axis ≈ boosted heavy particle

QCD jet τ_{-2} can also be small, but has a longer tail

Data and prediction agree

Similar results for R = 0.4 and for 90 < m_{jet1} < 100 GeV

Planar flow in backup

Multiple parton interactions – DØ

1 fb^{-1}
PRD 81, 052012 (2010)
PRD 83, 052008 (2011)

More than one parton-parton interaction from a single nucleon-nucleon collision

DP – double parton (two interactions)
TP – triple parton (three interactions)

Rates depend on PDFs and spatial distribution of partons within nucleon

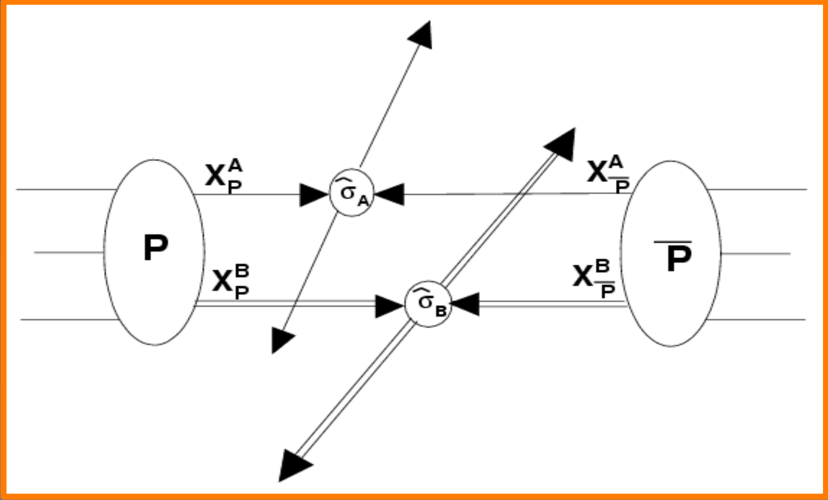

New and complementary information about proton structure

- spatial distribution of partons in proton
- parton-parton correlations

$$\sigma_{DP} = \frac{\sigma_A \, \sigma_B}{\sigma_{eff}}$$

σ_{eff} – describes the parton spatial density distribution

Background to rare processes with multi-jet final states

- SM Higgs
- SUSY

Uniform distribution – σ_{eff} large, σ_{DP} small
Clumpy distribution – σ_{eff} small, σ_{DP} large

Topology

Use γ + 2jet and γ + 3jet events

Signal – 1st interaction produces γ + jet
2nd produces jet + jet

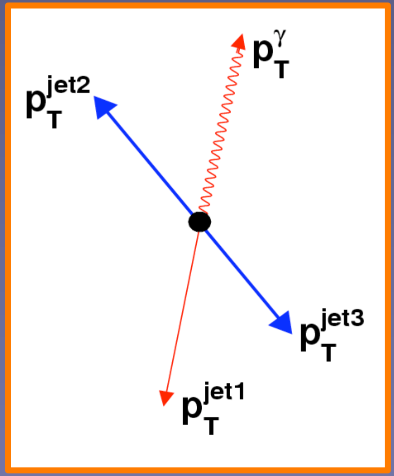

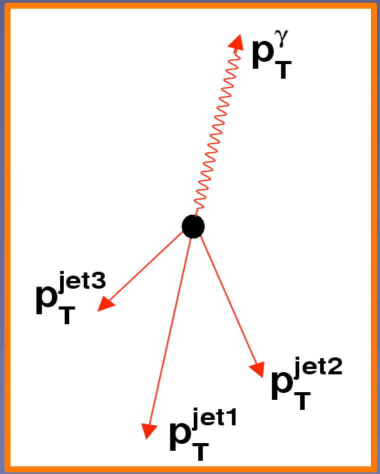

Background – γ + jet with two radiated jets
– two $p\bar{p}$ collisions

Binning in p_T^{jet2}
p_T scale of 2nd interaction

$50 < p_T^\gamma < 90$ GeV*, isolated
$|\eta^\gamma_{det}| < 1$, $1.5 < |\eta^\gamma_{det}| < 2.5$
$p_T^{jet1} > 30$ GeV
$p_T^{jet2/3} > 15$ GeV
$|\eta^{jet}| < 3.5$
$\not{E}_T < 0.7\, p_T^\gamma$
Single primary vertex
All pairs of objects $\Delta R > 0.9$

* $60 < p_T^\gamma < 80$ GeV (2010 analysis)

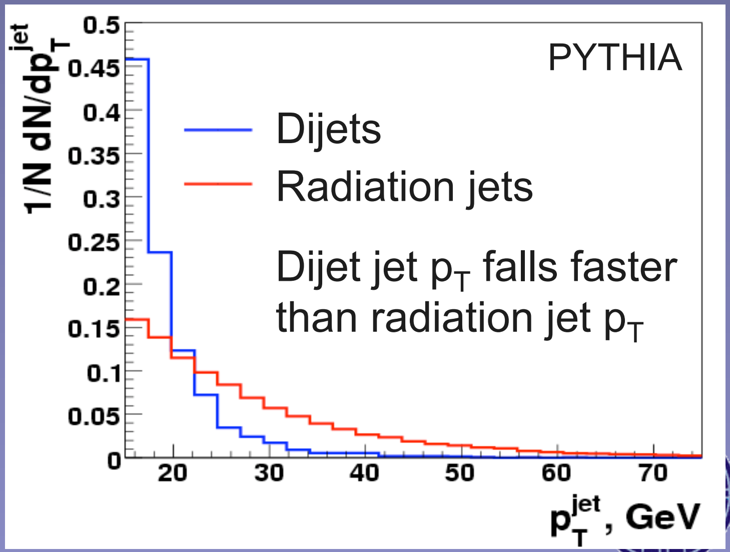

Discriminating variables

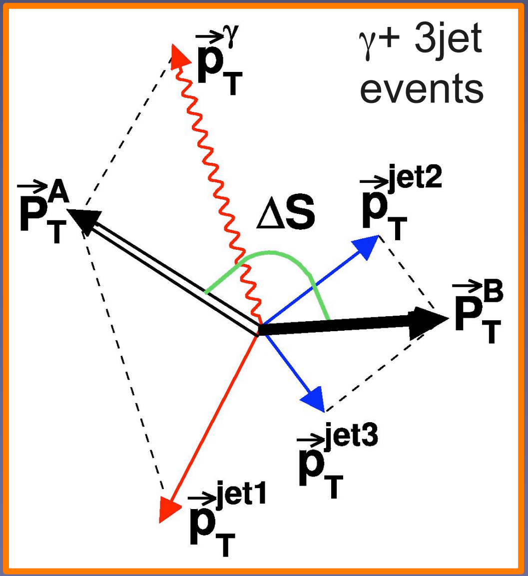

$\Delta S = \Delta\phi(p_T^{\gamma,jet1}, p_T^{jet2,jet3})$

(γ,jet1) and (jet2,jet3) are p_T-balanced pairs

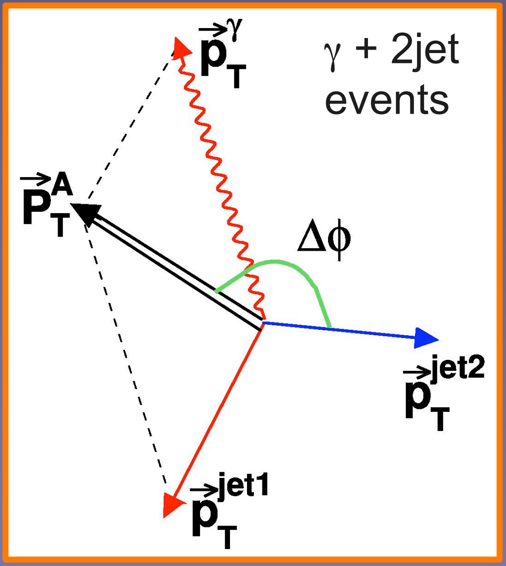

$\Delta\phi(p_T^{\gamma,jet1}, p_T^{jet2})$

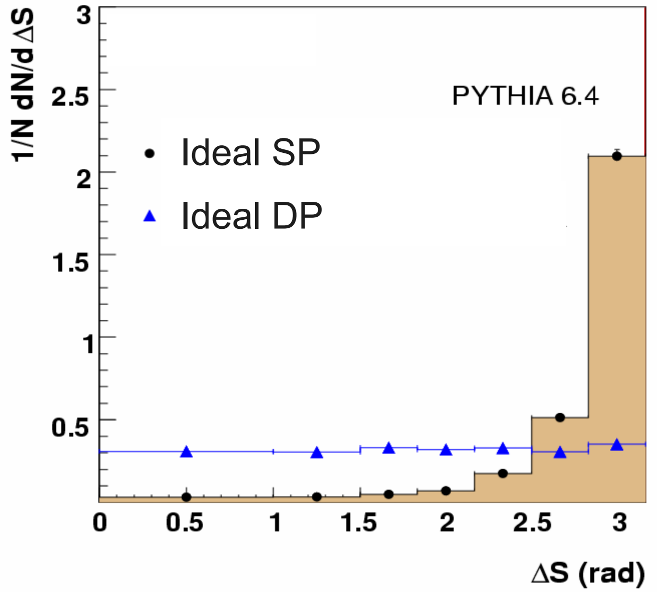

SP events peak at π

DP events flat

Since some jet1s are radiated, actually get bump at π for DP (jet1 doesn't go with the γ)

DP results

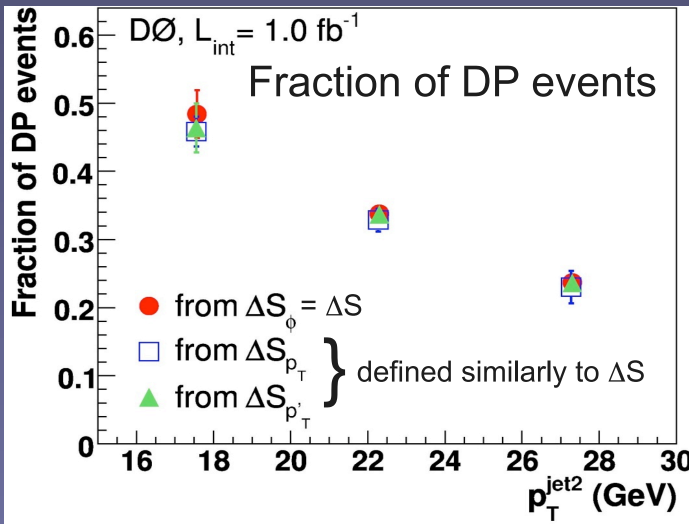

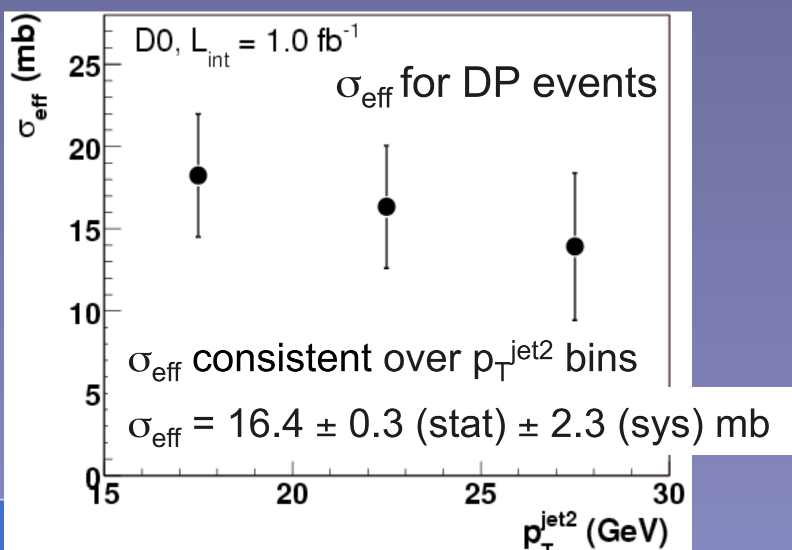

Comparison of differential cross section in data and various models, with and w/o MPI

MPI models with p_T-ordered showers are favored

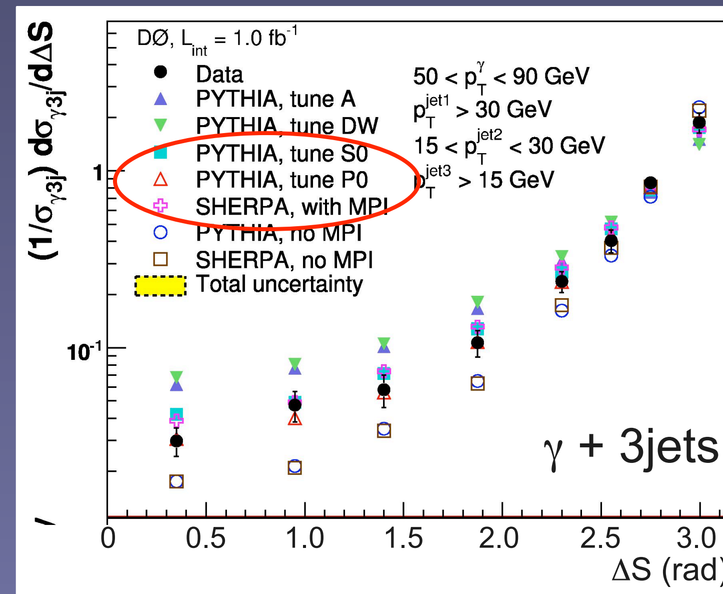

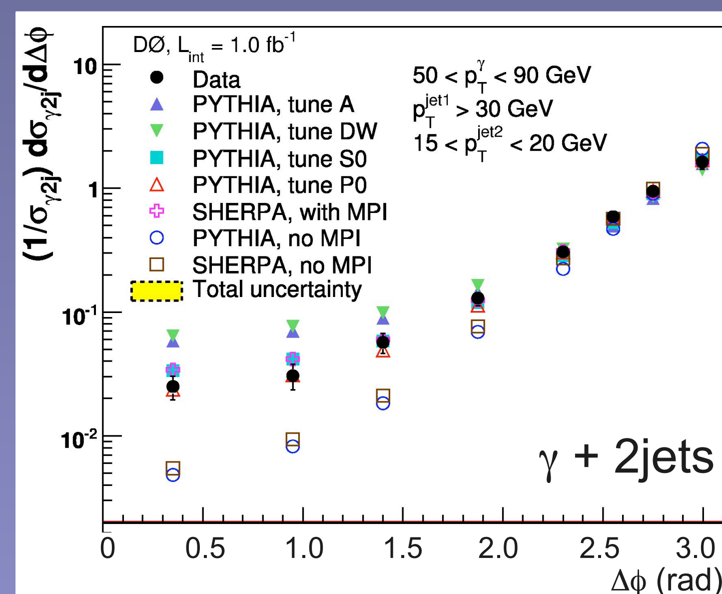

Summary

Measurements of photon pair production show none of the predictions is able to describe the data over the full kinematic region.

- $M_{\gamma\gamma}$ is best described, for masses above 80 GeV
- DØ finds the best agreement with RESBOS
- CDF with PYTHIA $\gamma\gamma$ + γjet

Data and PYTHIA predictions for high-p_T jet mass production and shapes agree, especially at high m_{jet}

Multiple parton interactions play a significant role and need to be included in simulations

- Measurements with γ + 2jets and γ + 3jets can be used to improve/constrain models

Many more results at

http://www-d0.fnal.gov/Run2Physics/qcd/

http://www-cdf.fnal.gov/physics/new/qcd/QCD.html

Backup

Corrections to particle level

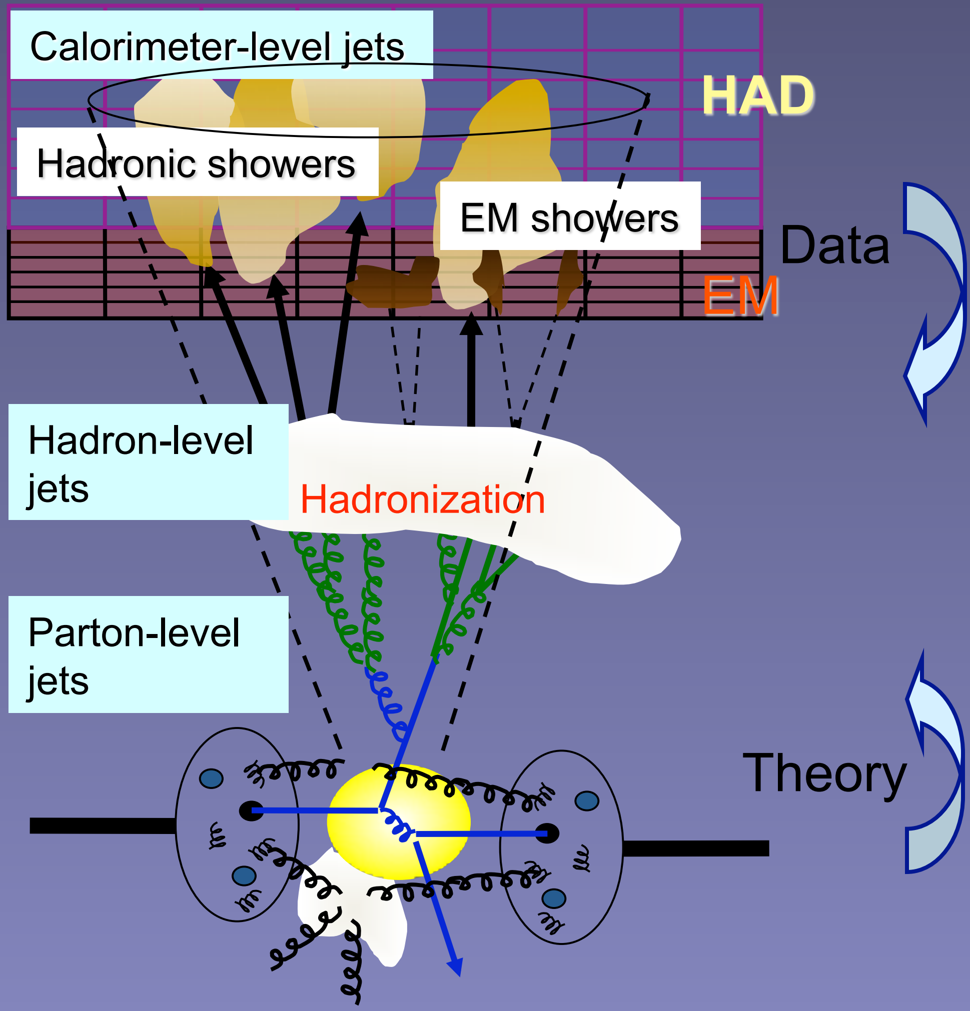

Most Run II jet results

- data are corrected to particle level including effects of underlying events and jet energy scale
- NLO theory is corrected to particle level using parton shower MC
- particle-level measurements are compared to particle-level NLO theory

Diphoton motivation

Many kinematic variables behave differently for QCD diphoton production and $H \rightarrow \gamma\gamma$ events; different dominant initial states – $q\bar{q}$ vs gg

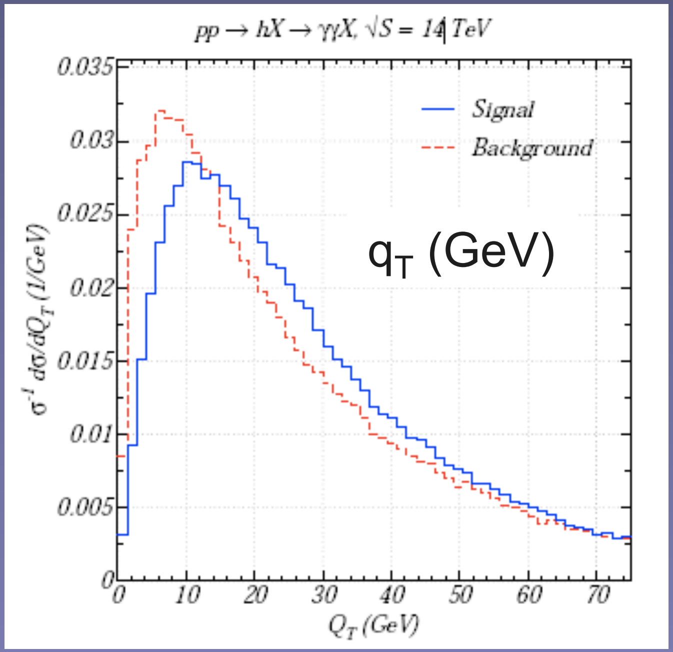

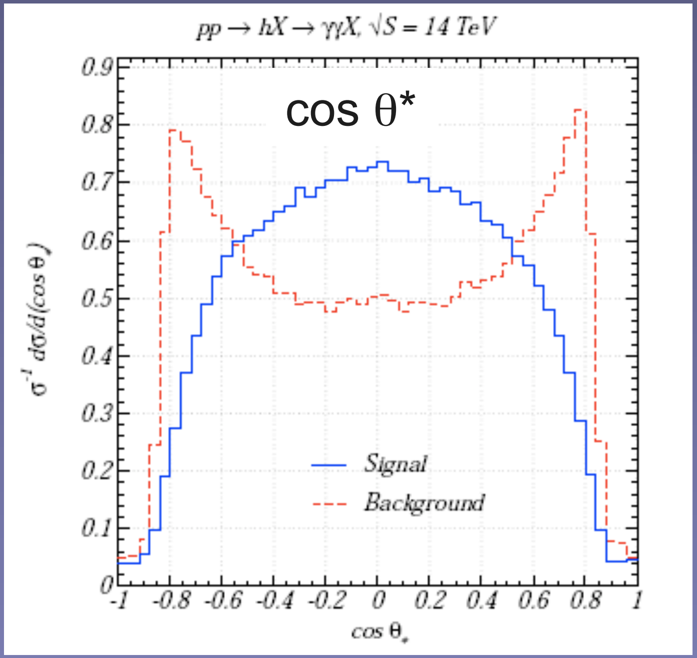

PRD76, 01309 (2007)

Use difference between diphotons from QCD and Higgs to improve sensitivity

Diphoton theory predictions DØ

- RESBOS and DIPHOX
  - CTEQ6.6M
  - all scales set to $M_{\gamma\gamma}$
    - renormalization, fragmentation, factorization
  - corrected for non-perturbative effects
    - underlying events, hadronization
    - using PYTHIA and two UE models
      - Tune A and S0
    - corrections are 4-5%, almost stable across bins of all observables (two tunes agree within 0.5%)

- PYTHIA v6.420
  - Tune A with CTEQ5L

- Uncertainties
  - PDF: 3-6%
  - Scale variation: 10-20%
    - factor of 2 up and down

Additional diphoton cross sections

Single differential cross section – CDF and DØ

$$\frac{d\sigma}{d(\cos\theta^*)} \qquad \frac{d\sigma}{d|\cos\theta^*|}$$

Single differential cross sections – CDF

$$\frac{d\sigma}{d\Delta\eta_{\gamma\gamma}} \qquad \frac{d\sigma}{d\eta_{\gamma\gamma}} \qquad \frac{d\sigma}{d\Delta R_{\gamma\gamma}} \qquad \frac{d\sigma}{d\log_{10}(p_T^{\gamma\gamma}/M)} \qquad \frac{d\sigma}{d\Delta y_{\gamma\gamma}/2} \qquad \frac{d\sigma}{dy_{boost}} \qquad \frac{d\sigma}{d(E_{T2}/E_{T1})}$$

$$\frac{d\sigma}{d(E_T)} \qquad \frac{d\sigma}{d\eta}$$

Double differential cross sections – DØ

$$\frac{d^2\sigma}{dM_{\gamma\gamma}\Delta\phi_{\gamma\gamma}} \qquad \frac{d^2\sigma}{dM_{\gamma\gamma}\, d|\cos\theta^*|}$$

$$\frac{d\sigma}{d|\cos\theta^*|}$$

$$\frac{d\sigma}{d(\cos\theta^*)}$$

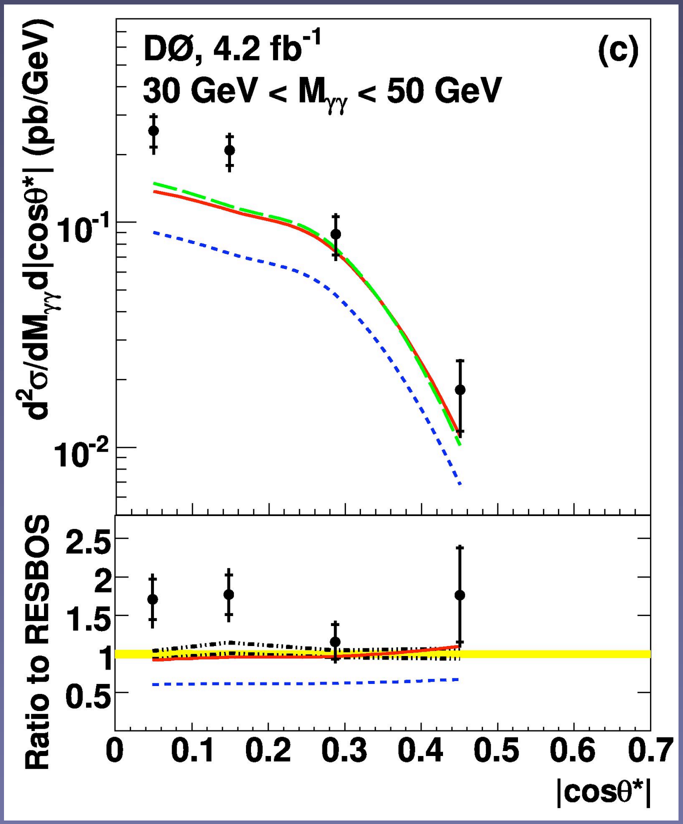

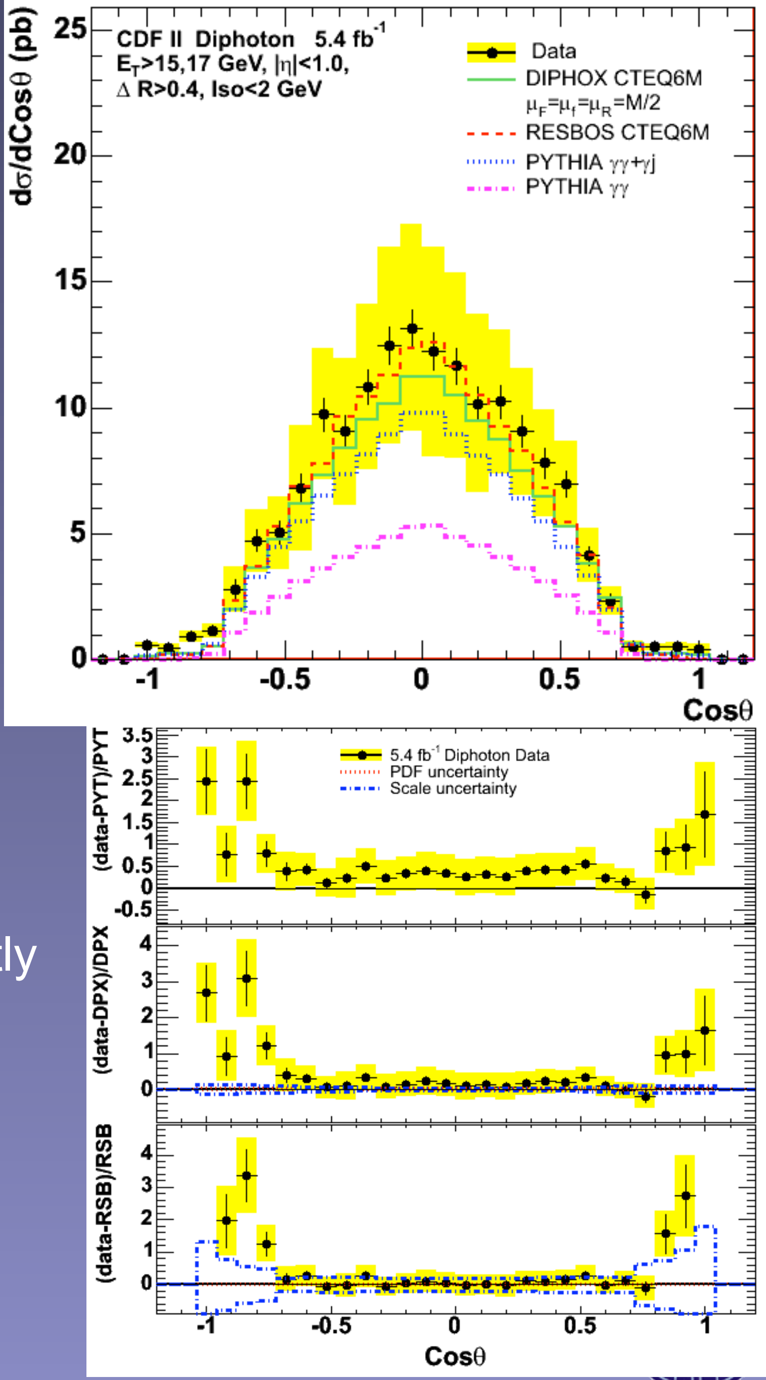

Cannot compare DØ and CDF measurements directly

DØ requires $p_T^{\gamma\gamma} < M_{\gamma\gamma}$

CDF does not

θ^* = polar angle in Collins-Soper frame

Susan Blessing

CDF γjet diagrams

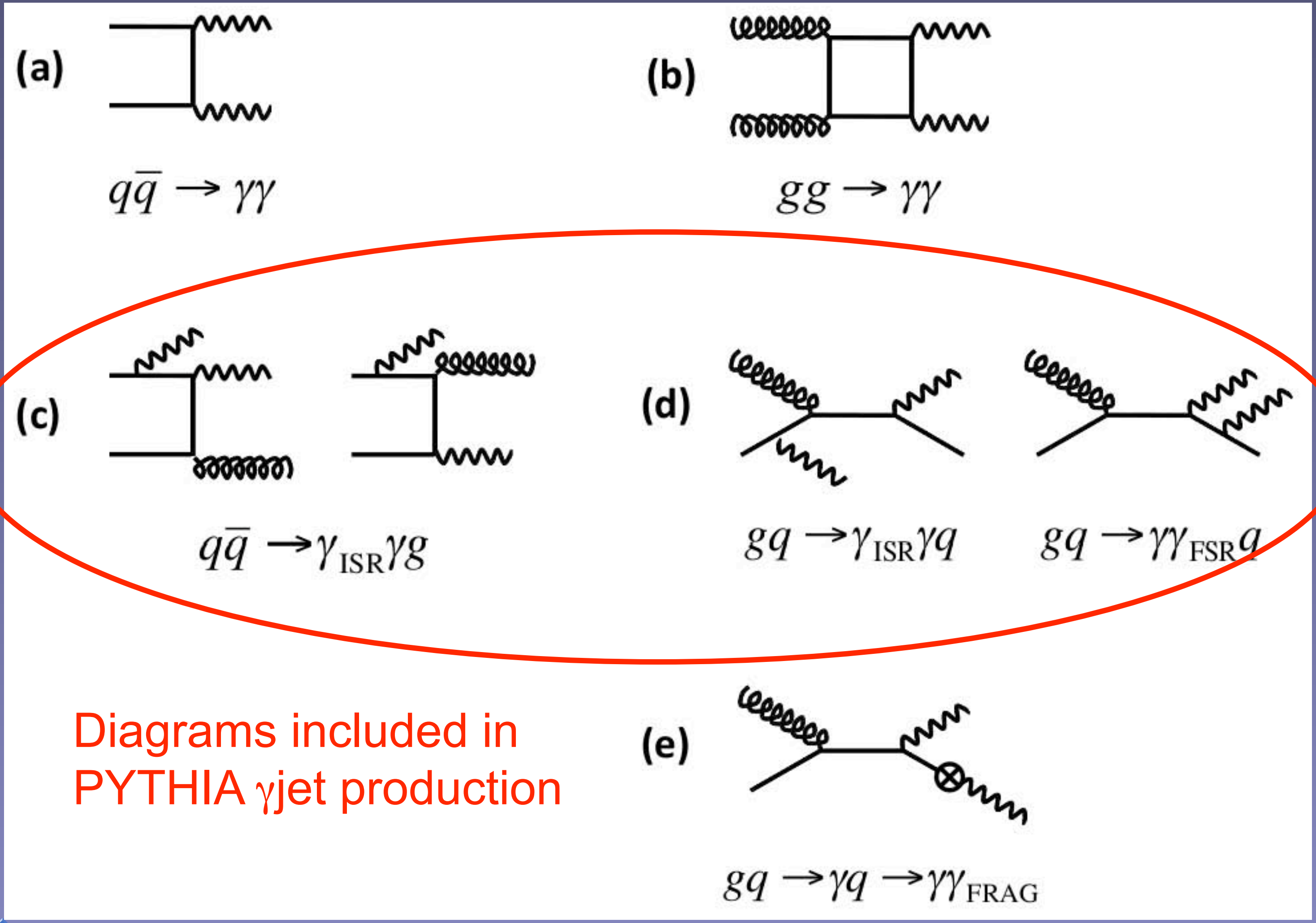

Diagrams included in PYTHIA γjet production

gg – DØ and Sherpa

SHERPA calculations (ME with up to 4 partons in the final state + PS) describe DØ data well

(F. Siegert, http://fsiegert.web.cern.ch/fsiegert/talks/2010-05-CMS-Hgg.pdf)

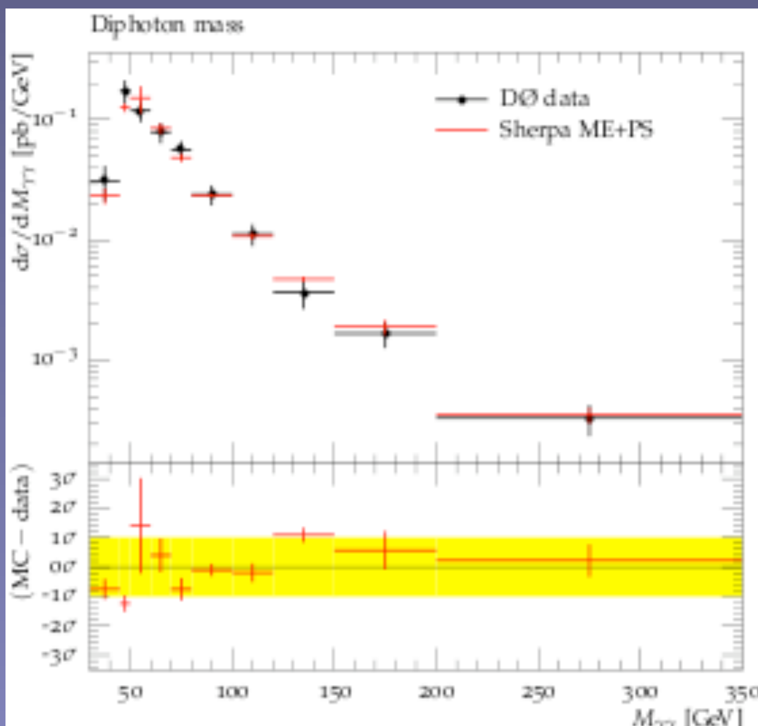

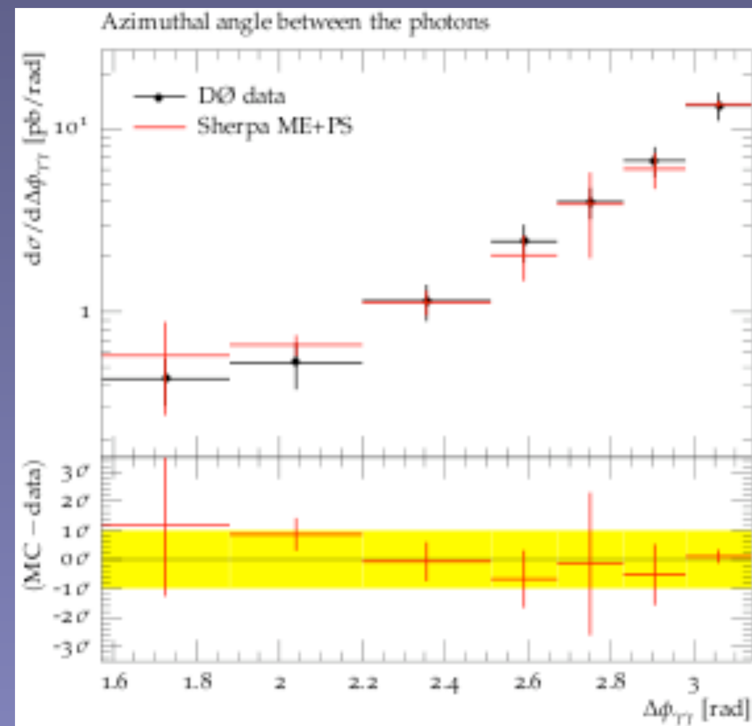

Angularity – QCD / Z comparison

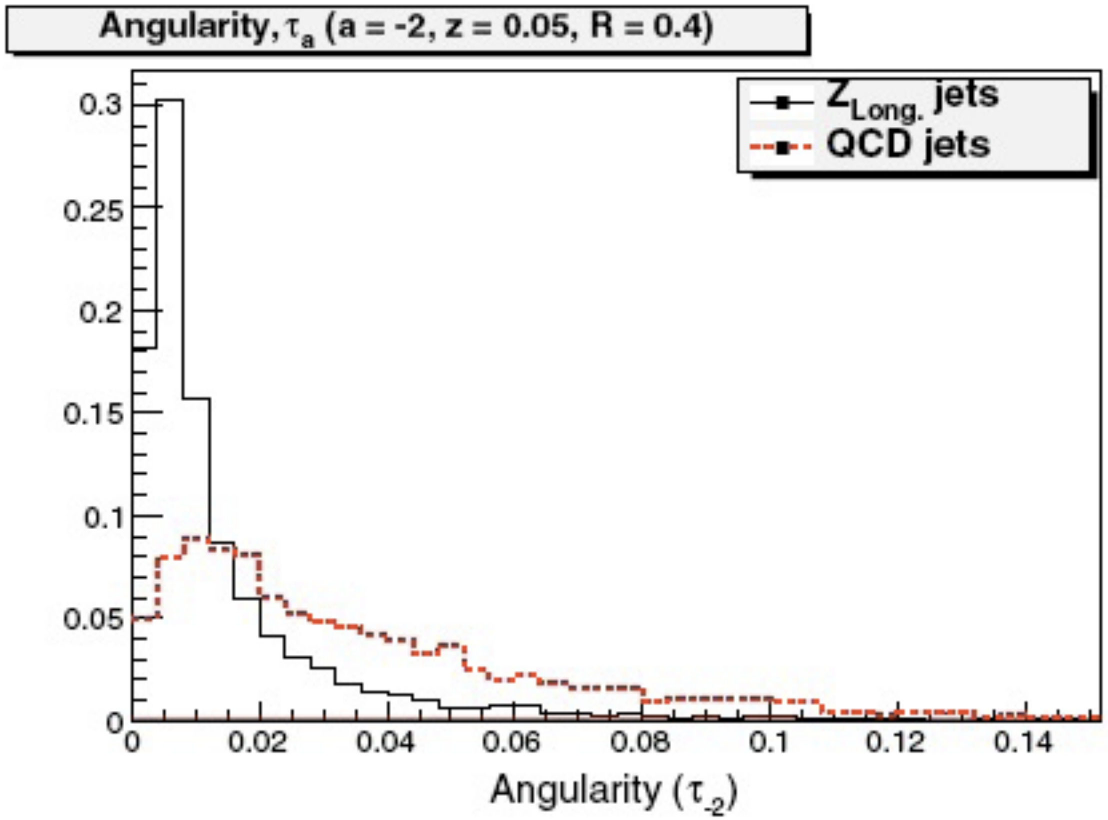

FIG. 4 (color online). The angularity distribution for QCD (red-dashed curve) and longitudinal Z (black-solid curve) jets obtained from MADGRAPH. Both distributions are normalized to the same area.

$$z = \frac{\min(p_{T1}, p_{T2})}{p_T}$$

Planar flow

Distinguish planar from linear configurations

Zero for linear shapes and 1 for isotropic energy distributions

$$P_f = 4\frac{\det(I_\omega)}{\mathrm{tr}(I_\omega)^2} = \frac{4\lambda_1\lambda_2}{(\lambda_1+\lambda_2)^2} \qquad I_\omega^{kl} = \frac{1}{m_{jet}}\sum_{i\in jet}\omega_i\frac{p_{i,k}}{\omega_i}\frac{p_{i,l}}{\omega_i}$$

IR safe

Independent of m_{jet}

$p_{i,k}$ – k^{th} component of p_T relative to the jet momentum axis

ω_i – energy of a jet tower (particle)

$\lambda_{1,2}$ – eigenvalue of the matrix I_ω

Monotonically increasing, but data steeper

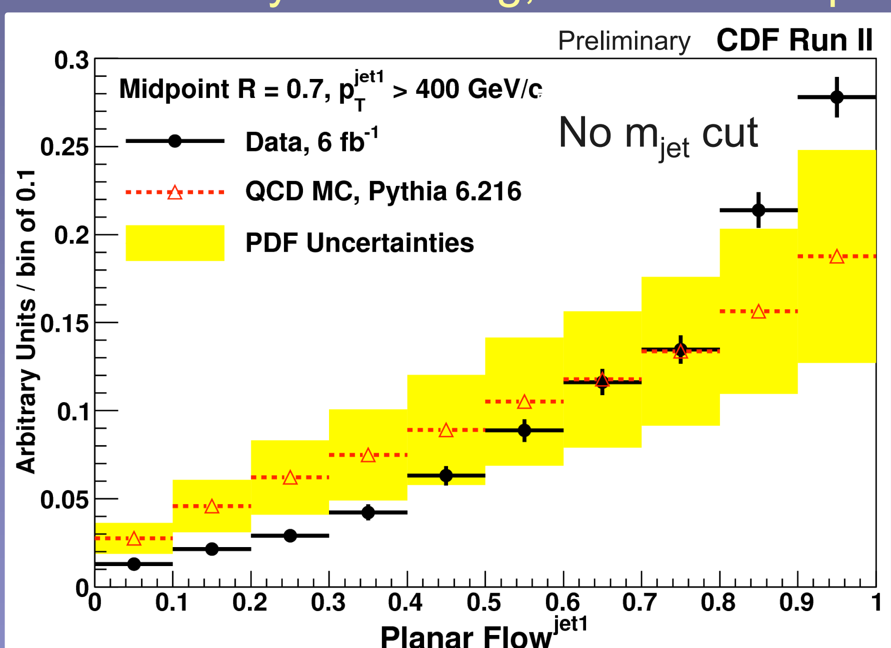

Agreement

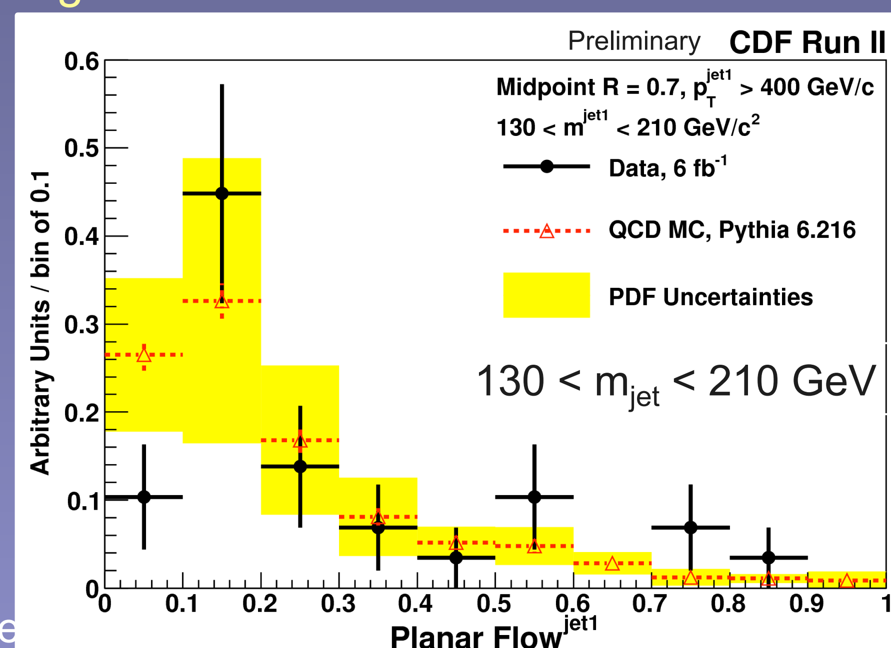

Planar flow – QCD / top jets comparison

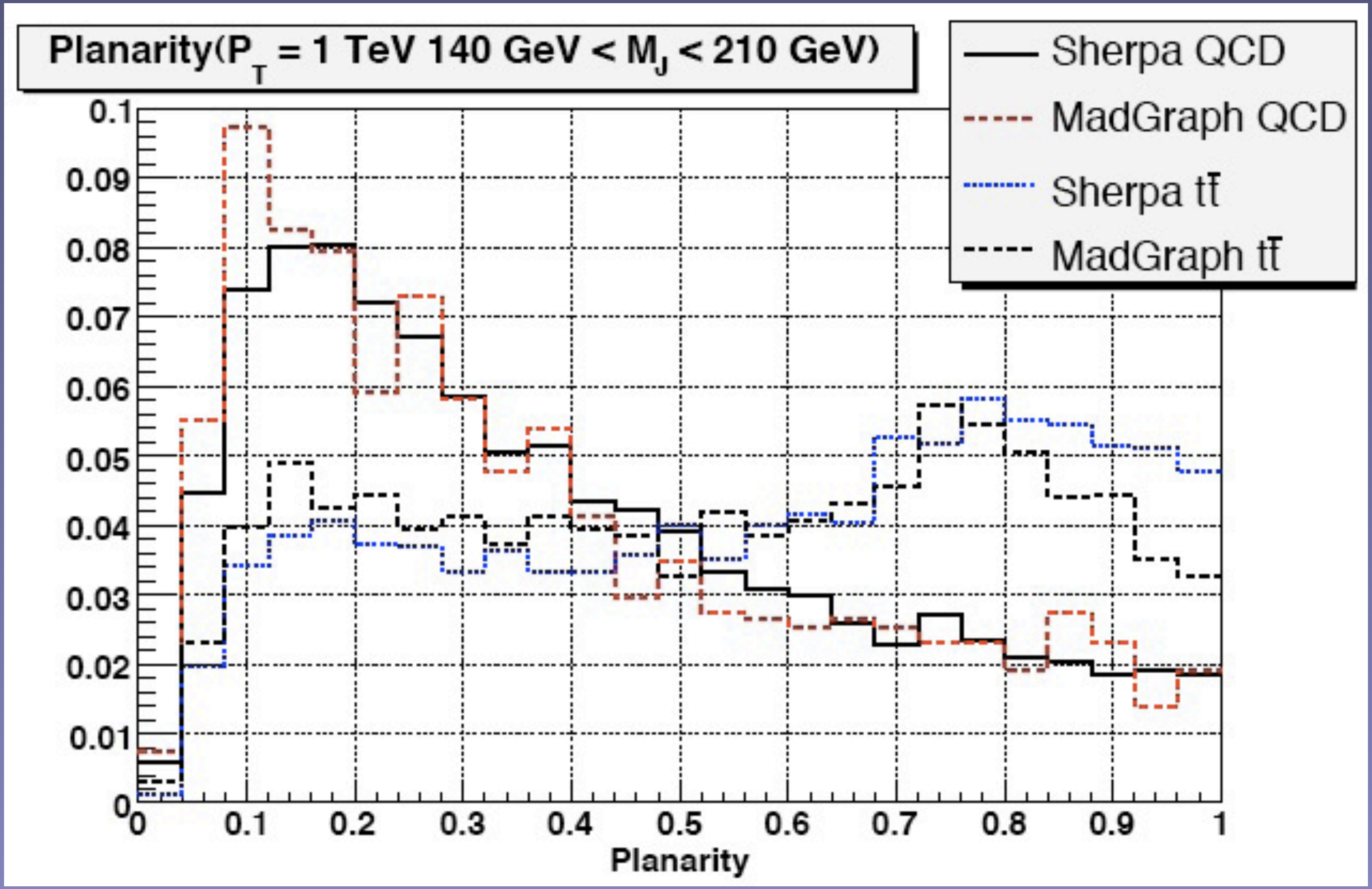

MPI

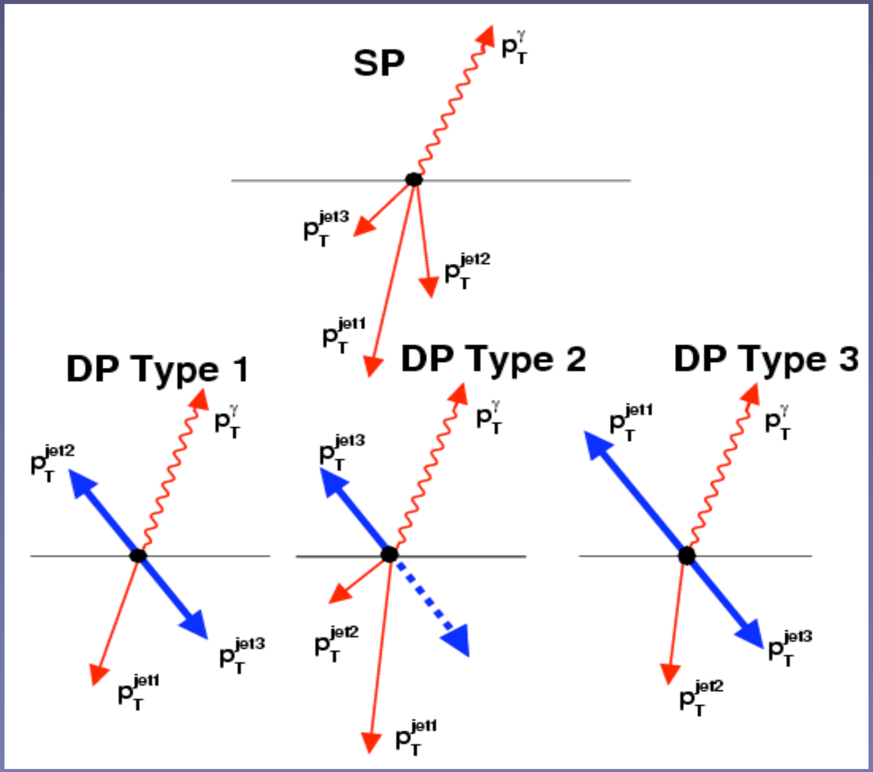

Ideal

Jet from dijet lost
Radiated jet observed

Jet from γjet lost
Radiated jet observed

MPI Data/MC

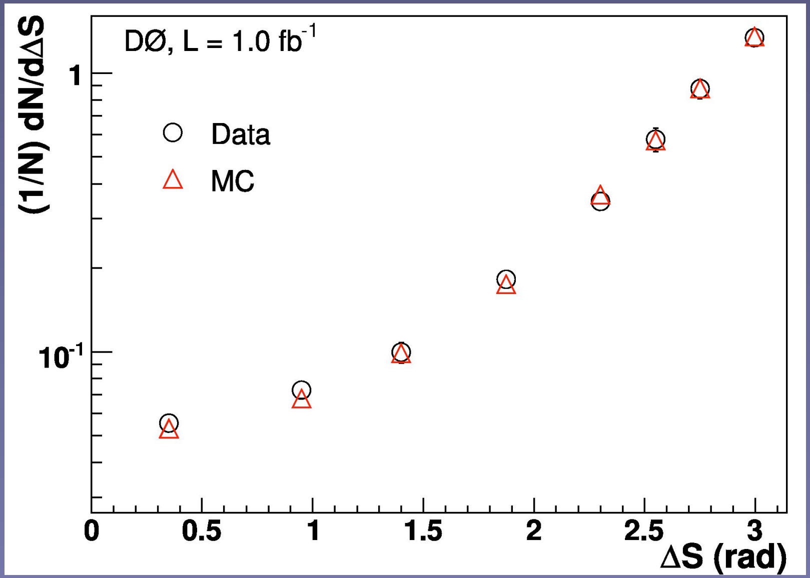

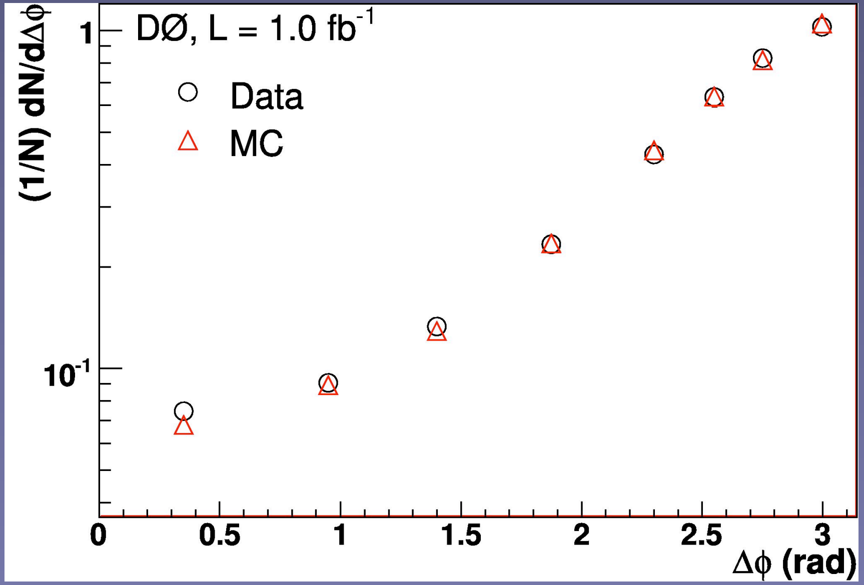

Data compared with MC reweighted to reproduce p_T^{γ} distribution in data for $15 < p_T^{jet2} < 30$ GeV

MPI differential cross sections

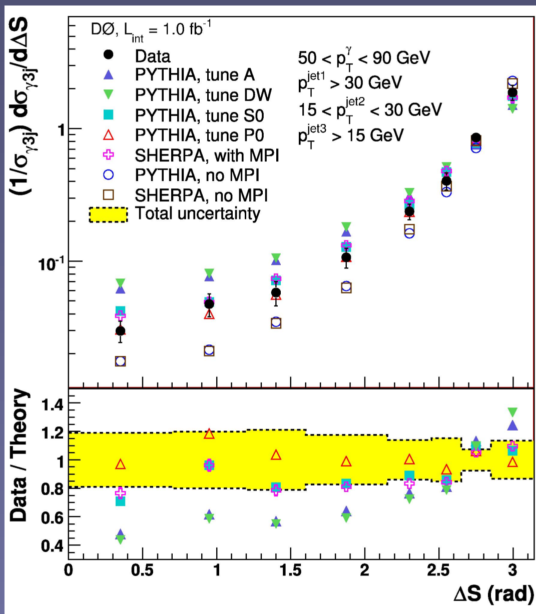

γ + 3jet

$15 < p_T^{jet2} < 30$ GeV

γ + 2jet

$15 < p_T^{jet2} < 20$ GeV, $20 < p_T^{jet2} < 25$ GeV, $25 < p_T^{jet2} < 30$ GeV